MICROBIAL MUTATIONS – ACCUMULATION IN MICROFLUIDICS AND COLLATERAL SENSITIVITY

by

Nathan Tyler Turner

A dissertation submitted to the faculty of
The University of North Carolina at Charlotte
in partial fulfillment of the requirements
for the degree of Doctor of Philosophy in
Bioinformatics

Charlotte

2023

Approved by:

_____

Dr. Way Sung

_____

Dr. Cynthia Gibas

_____

Dr. Rebekkah Rogers

_____

Dr. Jun-tao Guo

_____

Dr. Gang Chen

ABSTRACT

NATHAN TYLER TURNER. Microbial Mutations – Accumulation in Microfluidics and Collateral Sensitivity.
(Under the direction of DR. WAY SUNG)

Mutations are a primary source of genetic variation and a major driving force in evolution by influencing survivability (fitness), genetic disease, and the development of complex traits such as antibiotic resistance. However, studying the mutation process is extremely challenging and time consuming, as most mutation rates lie between 1×10^{-11} to 1×10^{-9} mutations per site per generation[1]. In my work, we have developed two major improvements in how we study the mutation process. First, we have developed a closed-system microfluidic platform that can be used to efficiently and rapidly measure mutation rates. This liquid-based platform overcomes many limitations of traditional growth methods and can allow for the study of extremophiles or pathogens that cannot be grown on solid media. Second, we are studying mutations that drive collateral sensitivity (resistance from one antibiotic giving rise to sensitivity from another antibiotic) within *Burkholderia multivorans* patient isolates. Across 8 lineages involving 6 antibiotics, we identify mutations in Chemoreceptor *CheD*, DNA ligase D, and BON domain-containing proteins that are associated with antibiotic sensitivity. These proteins are known to repair double-stranded DNA breaks and control efflux pump function, providing a mechanistic approach for combatting antibiotic resistant strains using gene therapy.

DEDICATIONS

This dissertation is dedicated to my lifelong friends, family and loved ones, all of whom have been a blessing and an honor to have in my life. I dedicate this to my parents and grandparents, Angie Poole, Eddie Turner, Phillis Poole, and Rallie Turner for their relentless support throughout my life as well as their tireless belief in me throughout my endeavors. It is no exaggeration to say that without my Maw-maw Rallie, I would have never made it into my PhD. This dissertation is also dedicated to my wonderful fiancé Brooke Watts, who has been my anchor and shared in both my worst days and best experiences through the entirety of my PhD, and who has never stopped believing in me even when I did not. This dissertation is dedicated to my closest friends who have been with me throughout my life and remain to be inspirations and lifelines when times get hard: Clay Whitworth, Ron Houser, Franklin Harris, Jacob Parks, Alec Heroux, and the numerous others who have supported me throughout my life and will always be there when times get hard.

In addition, this dissertation is dedicated to the loving memory of those who have sadly been taken from us far too soon. I dedicate this dissertation to my two grandfathers, Walter Poole, and Charles Turner. Not a day goes by without them in my thoughts while continuing to try and honor their name, you are sorely missed. Finally, I dedicate this dissertation to Dr. Miroslaw Mystkowski, Professor of Computer Science at Gardner-Webb University. Your patience, knowledge and understanding have truly been an inspiration, and it has been an honor to be your student and friend.

ACKNOWLEDGMENTS

This Doctoral dissertation is dedicated to all those in my life who always believed in my ability and desire to accomplish my goals. I would like to thank Dr. Way Sung, who without his acceptance and opportunities given, I would have never been able to produce the research and technologies I have. For that, I am truly thankful. I would also like to thank Dr. Anita Rana, and David Patton along with the other members of the Sung lab who throughout my PhD have always been there for advice and support, even when dealing with things beyond the scope of their own work, I am truly blessed to have been a part of such an amazing team. I would like to thank Dr. Rebekah Rogers and the members of her lab for the company they have kept during the long hours in the lab and the numerous journal club experiences and get-togethers we shared outside of work.

I also owe a great deal of thanks to my academic advisor Dr. Cynthia Gibas, who has always made time to hear any problems or concerns that would arise throughout my time spent here and was always supportive of my interests. I would like to thank the members of my committee, Dr. Jun-tao Guo, and Dr. Gang Chen for their time and willingness to be on my committee and help guide me through these final steps as I move on to the next phase of my life. Finally, I would like to thank anyone not mentioned above who has been a significant part of my life or been supportive of me along the way. No matter how small the assistance or time spent was, it did not go un-noticed and I am truly thankful for everyone who helped me get to where I am now, I could not have done this alone and I thank you from the bottom of my heart.

Table of Contents

List of Tables

List of Figures

List of Abbreviations/Terms/Jargon

DNA	Deoxyribonucleic acid
MA	Mutation Accumulation
PDMS	Polydimethylsiloxane
WGS	Whole genome sequencing
dS	Synonymous site
dN	Non-synonymous site
Ne	Effective population size
BFM	Bacterial flagellar motor
FFF	Fused Filament Fabrication
PLA	Poly lactic acid
SLA	Stereolithography
UV	Ultraviolet
CAD	Computer-aided design
STL	Stereolithography
INDEL	Insertion/deletion mutation
BCC	*Burkholderia cepacia* complex
CF	Cystic Fibrosis
CFTR	CF transmembrane conductance regulator
MDR	Multi-drug resistance
CS	Collaterally sensitive
CR	Collateral resistance
TD	Treatment drug
MIC	Minimum inhibitory concentration
NTD	Non-treatment drugs
LB	Lysogeny broth
ZOI	Zone of inhibition
GFF	General feature format
CHL	Chloramphenicol
CAZ	Ceftazidime
MEM	Meropenem
MIN	Minocycline
LVX	Levofloxacin
SXT	Trimethoprim-sulfamethoxazole
βLA	Beta-lactam

Chapter 1: Introduction, Significance & Background

Significance:

Understanding mutations and their rate of formation is critical in gaining insight on how an organisms mutate and evolve. Mutations drive evolution in that they are a primary source of genetic variation that can lead to differences between two organisms within a species[2]. In bacteria, mutations have been linked to the development of antibiotic resistance[3], pathogenicity[4-6], and the evolution of new bacterial traits and species[7-9]. In humans, mutations have been associated with many types of genetic diseases including cystic fibrosis, hemophilia, and to an extent, even certain types of cancers[10, 11].

In phylogenetics, mutation rates are extremely useful in determining how long ago two species diverged from one another. This concept is referred to as the molecular clock[12]. If we assume that mutations arise at a relatively constant rate over time, the mutation rate per generation can be used to determine how long it has been since any given species has diverged from a common ancestor [13]. These studies can be beneficial across all clades of life and can help improve our overall understanding of previously less studied species.

In addition, mutations can impact the fitness and genetic content in an organism[14, 15]. Small-scale mutations such as insertions, deletions, and base substitutions can arise in a gene, leading to changes in protein structure and function. Large-scale mutations such as segmental deletions and duplications can impact many genes at once and can have a large impact on the evolution of genome architecture within an organism. These fitness effects that arise from mutations play a major role in determining an organisms fate as well as frequency of distribution

within a given population[14]. These phenomena can be studied through an experimental process known as mutation accumulation.

Mutation accumulation (MA) experiments are a time-tested method used to study the rate of spontaneous mutations within an organism. Through repeated bottlenecking, the MA process aims to reduce the efficiency of selection over the lifetime of the experiment, allowing for the accumulation of all but the most deleterious mutations. However, traditional MA experiments are mostly performed on solid media [16-20]. There are a few major limitations of using solid media for MA. First, because mutation rates are extremely low (1×10^{-11} to 1×10^{-9} mutations per site per generation) [21], these experiments take a considerable amount of time as it takes a large number of generations in order to accumulate a significant number of mutations (3000-5000 generations). Second, a majority of bacteria cannot be cultured on solid media, including over 99% of all bacterium [22]. Third, bottlenecking organisms on solid media is extremely time consuming and costly, generating large amounts of waste (e.g., petri dishes and liquid media) [23].

Despite the need for a greater understanding of the mutation process, our ability to conduct large-scale mutation assays remains limited. Prior work has shown some success in conducting large-scale mutation accumulations studies using microfluidics. In this work, the authors create bacterial bottlenecks using tiny microfluidic channels to trap and isolate cells [24, 25]. While these studies were able to determine the rate of spontaneous mutations in mismatch-repair deficient *Escherichia coli* these studies have major limitations including the inability to discern between mutational types, and the inability to handle species with varying cell sizes.

Objectives and Innovation

The overall goal of this project was to design a microfluidics device that can generate an effective bottleneck across multiple lineages simultaneously and be flexible enough to handle different microbial species. This microfluidic platform can be utilized to rapidly generate an unbiased estimate of the rate and spectrum of spontaneous mutations for mutation studies while overcoming the limitations of prior methods [25, 26]. In addition, the device should be as cost-effective and adaptable as possible for ease of use and implementation.

There are three major innovations in this project. First, this microfluidic platform allows for the growth, bottlenecking, and collection of many cellular types. Although other microfluidic platforms allow for bacterial growth, this platform is unique in that it can bottleneck cells of any size, the cells are collectable, and then can be used in down-steam sequencing.

Second, this platform is designed to be low-cost. In the past microfluidic platforms have been created using a material known as PDMS or polydimethylsiloxane which is a type of silicone that is very commonly used in microfluidics due to its durability and accuracy [27]. However, many PDMS molds can be very costly, so modifications are costly and time consuming, and have limitations in their design due to the manufacturing process.

Third, due to the low-cost nature of this platform, this microfluidic platform can be repurposed or redesigned to be used in many different experiments outside of mutation rate measurements. For example, slight modifications in this platform can allow this platform to be used to study microbial population dynamics, as well as more complicated processes such as horizontal gene transfer.

Background

Mutation Rate Estimation, prior studies and History

Mutation rate estimation is an essential part of understanding the process of natural selection and evolution. Mutations are a primary source of genetic variation and their fate is determined by evolutionary forces such as natural selection and genetic drift [28]. Studies on mutation rates have been conducted for over a century, and methods to estimate mutation rates have improved significantly throughout this period of time. This section describes past and present methods used to measure mutation rate.

Prior studies on mutation fitness effect

Gordo et al. discusses some of the most important findings with mutations and their effects, including the various ways in which bacteria are able to generate variety on a genetic level[14]. It I known that mutations can produce a wide range of effects from organism to organism, which can be either beneficial, neutral, or deleterious. Beneficial mutations are any mutations that occur which create some change in genetic makeup that leads to a positive effect on fitness. Examples of these types of effects include antibacterial resistances within bacteria. These beneficial effects tend to be seen more frequently in bacteria when they are placed within a stressful environment[14]. Neutral mutations are any mutations that occur that are neither beneficial to the organism nor deleterious to it. These can include mutations which create synonymous effects within triplets that ultimately do not alter the generated codon, called silent mutations. Deleterious mutations are the remaining mutations which cause any change in genetic makeup leading to a decrease in the fitness of an organism, and are thought to be the largest

representation of mutations[29]. It is still a topic of discussion as to the frequency and proportion that each type of mutation occurs. There are a number of experiments which suggest that in microbial studies, beneficial mutations arise more frequently that is to be expected[30]. On the other hand it can be incredibly challenging to distinguish between mutations with are mostly neutral or have only a slightly deleterious effect on an organism [14].

Luria- Delbrück

In one of the earliest mutation rate estimates, Luria and Delbrück [31] conducted what is now called a fluctuation assay, whereby a large number of parallel cultures are inoculated with the bacteria of interest. After reaching saturation they are then plated onto selective media that the wild-type bacteria cannot survive on. However, mutations in certain genes will allow the bacteria to survive on the selection media. By counting the number of bacteria that survive on selective media and contrasting that to those who survive on nonselective media, one can estimate the mutation rate. Repeated measurements will allow for a rough estimation of the mutation rate at that locus and can then be extrapolated to the mutation rate over the genome [32].

The calculation is given by:

$$\left(\frac{\bar{r}}{m}\right) - \ln m - \ln(C) = 0$$

where $\bar{r}$ is the mean number of mutants in a culture, m is the number of mutations per culture, and C is the number of cultures in an experiment [32].

There are numerous benefits to the fluctuation assay experimental design, one of which being its broad application to different organisms. Furthermore, fluctuation assays are extremely rapid and quick to perform. Another positive factor with fluctuation assays is that they are designed to maximize precision in terms of estimating the mutation rate. Although fluctuation assays can give a rough estimate mutation rate in an organism, there are some major limitations to this method. First, an accurate calculation of mutation rate will heavily depend on the value of m. If the value of m is too low, then the estimation will be inaccurate. If the value of m is too high, too many bacteria will be able to survive the selection media. Furthermore, different loci are subject to differential mutation rates based upon GC-content, and phenotypic lag, where survival and growth on selective media is reduced or delayed [32].

Reporter Construct

Reporter construct, otherwise known as a reporter gene, allows us to track the biological processes of gene expression and gene interaction. A reporter constructs is that an easily traceable gene segment can be placed into a genome, amplified, and then sequenced after some period of time [33] in order to study any mutations that occur.

Benefits of reporter constructs include a wide range of fluorescent proteins which can be used in a multitude of bacterial studies [33]. Commonly used reporter genes include: Luciferase, β-Galactosidase, β-Glucuronidase, Secreted alkaline phosphatase, and Green Fluorescent Protein

[34-38] and have broad applications from mammalian studies to single cell organisms such as bacteria and yeast [39]. Rapid detection of gene expression is also possible thanks to the immediate visual distinction between colonies with fluorescence factors. On the other hand, the formation of these fluorophores can develop slowly, and the final steps require molecular oxygen, which limits its application to aerobic environments [33]. Due to the specificity required of the reporter construct, it can be both costly and time consuming to engineer the desired reporter construct for a given organism. Additionally, single gene content might not match whole genome content, producing limited or even misleading outcomes.

Phylogenetic Estimation

Trios

Human trio studies involve a direct analysis of mutations that arise from the immediate offspring of two individuals, typically through whole genome sequencing (WGS). The benefit of these studies is that it becomes possible to track direct mutations in a single generation. While human Trios studies do provide insight on direct tracking of mutations within a set number of generations there are some inherent drawbacks. One of the most significant shortcomings is the lack of mutations across the experiment, particularly in organisms with low mutation rates per site per generation and a small genome size, and the sequencing costs associated with assaying a

small number of mutations. Furthermore, studies have also shown that these mutations found can be highly variable even within a single parent/child trio [40].

Previous studies with human trios have revealed information on the variation of mutational rates even within a closely related family. Sasani et al. published a study in which they analyzed the genetic information produced from sequence data from 33 large, three-generation CEPH families[41]. They concluded that there was significant variation in the effects of parental age on de novo mutations within their offspring, which ranged from 0.19 to 3.24 de novo mutations per year[41]. Of the mutations that were studied, roughly 10 percent of all de novo mutations were post-zygotic and found in both the somatic and germ cells, demonstrating that post zygotic mosaicism is a significant source of human mutations[41]. Additionally, they mention that parental age plays a critical role in the frequency of newly arising mutations within each generation as seen in figure 1.

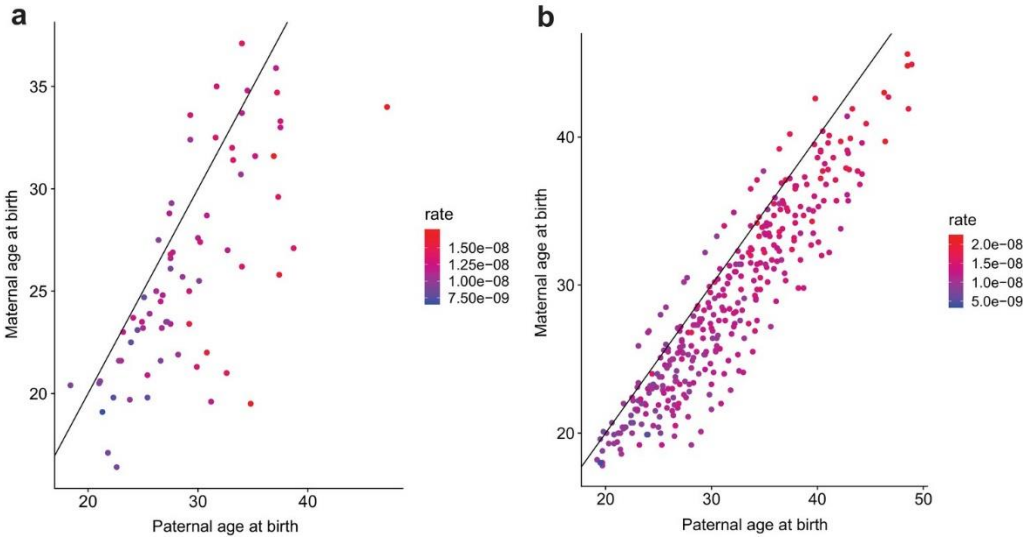

Fig 1. (a) second generation and (b) third generation individuals in the study cohort. Each plot shows relationship between parent age at birth, point colors represent magnitude of mutation rate[41].

Synonymous site changes

There are two broad categories for studying mutations in humans, direct tracking through mutation accumulation lines (see below), reporter constructs, or trios, or indirect methods which "infer mutation rates in levels of genetic variation within or between species" [40]. Understanding how selective pressures work on an organism is critical in gaining insight into the evolutionary process. If a species is to evolve, then it should be understood that "adaptation should induce more genetic changes at amino acid altering sites in the genome, compared to amino acid–preserving sites [42]." The dN/dS ratio was developed to measure selective constraint [43]. By understanding the substitution rates at both synonymous, or silent sites due to the redundancy of the genetic code, and non-synonymous sites we can reach a better understanding of the adaptation that is occurring within an organism. This ratio was originally developed to study distantly diverged species but with the rise of sequencing technologies, is generally applied to sequence samples from a single species [42]. The changes at synonymous sites (dS) are often used as a proxy as mutation rate, as neutral silent sites (amino acid preserving changes) are assumed to evolve at the rate of mutation. However, Selection has been shown to occur at silent sites in both eukaryotes and prokaryotes, which can bias the estimate of mutation rates based upon dS.

Mutation Accumulation

State-of-the-art methods for measuring mutation rates involve mutation accumulation (MA) lines. The process of a MA experiment involves taking an organism and repeatedly bottlenecking it, by transferring it to a new, identical environment to propagate. The equation for the probability of fixation of a single mutation in a population with effective population size N_e, and census population size of N is given by Kimura(1962) is as follows $su(s) = \frac{2s\left(\frac{N_e}{N}\right)}{1-e^{-4N_e s}}$ [44]. As the effective population size is effectively 1, $N_e s$ is effectively negligible, meaning that the probably of fixation of mutations in a bottleneck is equal to the rate of mutation. Additionally, as effective population size (or the number of organisms contributing to the gene pool of the next generation) is low, the fate of new mutations are determined by random genetic drift [45]. In an long-term MA experiment, mutations are accumulated in an unbiased fashion, and whole-genome sequencing can be used on any of the lineages to provide information on the number of mutations, where they occurred, and what types of mutations are present [46]. These mutational rates can be calculated by the following equation:

$$u = \frac{r_2}{N_2} - \frac{r_1}{N_1} \Big/ \ln\left(\frac{N_2}{N_1}\right)$$

Where r is the number of mutants and N is the number of total cells, which are determined at various points during the growth of the cultures during the experiment, and assuming no difference in growth rate then the mutation rate u is simply the slope of the line of r versus the total number of generations [32].

There have been many MA experiments performed in the recent years, with studies covering a broad spectrum of organisms and species [47-52], all of which provide helpful insight into the evolutionary process.

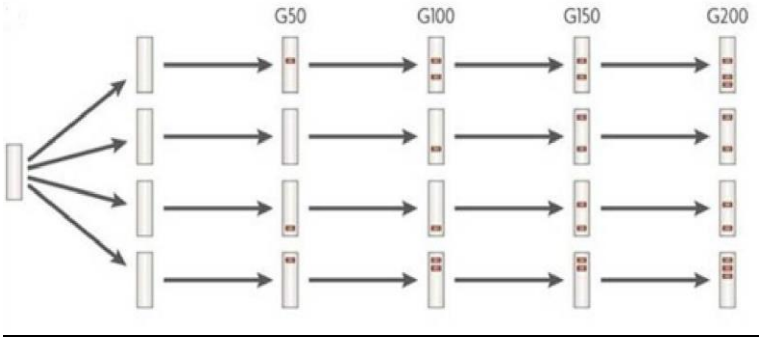

Figure 2: Mutation accumulation and Bottlenecking – Mutation Accumulation occurs by taking a single ancestral organism and establishing multiple MA lines, which are repeatedly propagated by selecting a single offspring in a new environment repeatedly allowing an unbiased accumulation of mutations. Illustration by Baer et al., Nature Reviews: Genetics 2007.[53]

MA lines

MA lines that have been completed:

Species	Gen.	Lines	Species	Gen.	Lines
Agrobacterium tumefaciens C58	5819	47	Mycobacterium smegmatis MC2	4900	49
Arthrobacter sp. KBS0703	5194	58	Rhodobacter sphaeroides 17025	4544	46
Bacillus subtilis NCIB 3610	5077	50	Ruegeria pomeroyi DSS-3	5386	47
Burkhoderia cenocepacia HI2424	5554	47	Staphylococcus aureus 25923	2716	83
Caulobacter crescentus NA1000	4284	44	Staphylococcus epidermidis	7101	22
Colwellia psychrerythraea 34H	1078	84	Teredinibacter turnerae T7901	3025	42
Deinococcus radiodurans BAA-816	5961	43	Vibrio cholerae 2740-80	6453	46
Escherichia coli K-12 MG1655	1682	46	Vibrio fischeri ES114	5187	48
Flavobacterium sp. KBS0721	5940	43	Burkholderia multivorans [CHL]		20
Gemmata obscuriglobus DSM5831	2336	41	Burkholderia multivorans [LVX]		44
Janthinobacterium lividum KBS0711	5023	49	Burkholderia multivorans [MEM]		72
Kineococcus radiotolerans SRS30216	4724	44	Burkholderia multivorans [MIN]		34
Lactococcus lactis DSMZ20481	3973	63	Burkholderia multivorans [SXT]		47
Mesoplasma florum L1	2351	28	Burkholderia multivorans [CAZ]		62
Micrococcus sp. KBS0714	3834	60			

Table 1: MA lines that have been completed by Long and Sung[54]. Each species is listed along with the total number of generations achieved, and how many total cell lines were conducted.

It is from these lines that have been completed that we are able to gain a better understanding of mutational rates, as well as the impact that mutations have on several organisms. The realm of evolutionary biology is still limited in its total understanding of the underlying factors as to why mutations arise and the frequency in which they do so. Thankfully, new studies are constantly being produced to increase our knowledge and better shape a wholistic picture of the underlying evolutionary process.

Mutation Rate Evolution

Drake's Rule

One challenge with population genetics is that understanding the evolutionary forces of drift and selection requires assumptions regarding the rate of evolution (mutation rate) at different sites. In 1991, John Drake postulated that "within broad groups of organism, the density of accumulated mutations per generation is roughly inversely proportional to genome size, which can vary by a few orders of magnitude [55]." The purpose of this study was to help establish an understanding of the mutational process and how mutations come to rise. These mutational rates

are known to vary greatly both within and across organisms. Drake was able to estimate a mutational rate for several organisms shown in table 2.

Organism	Genome size, bp	Target	Mutation rate: Per bp (μ_{bp})	Mutation rate: Per genome (μ_g)
Bacteriophage M13	6.41×10^3	*lacZα*	7.2×10^{-7}	0.0046
Bacteriophage λ	4.85×10^4	*cI*	7.7×10^{-8}	0.0038
Bacteriophage T2	1.60×10^5	*rII*	2.7×10^{-8}	0.0043
Bacteriophage T4	1.66×10^5	*rII*	2.0×10^{-8}	0.0033
E. coli	4.70×10^6	*lacI*	4.1×10^{-10}	0.0019
			6.9×10^{-10}	0.0033
		hisGDCBHAFE	5.1×10^{-10}	0.0024
S. cerevisiae	1.38×10^7	*URA3*	2.8×10^{-10}	0.0038
		SUP4	(7.9×10^{-9})	(0.11)
		CAN1	1.7×10^{-10}	0.0024
N. crassa	4.19×10^7	*ad-3AB*	4.5×10^{-11}	0.0019
		mtr	(4.6×10^{-10})	(0.019)
			1.0×10^{-10}	0.0042
		Median excluding outliers		0.0033
		Arithmetic mean excluding outliers		0.0033
		Geometric mean excluding outliers		0.0031

Table 2: produced by J W Drake. “Rates of spontaneous mutation in DNA-based microbes.” This table displays the estimated mutation rates of multiple organisms found in his publication[56]

What Drake concluded based on his findings was that most organisms across microbial species had a mean mutational rate of 0.0033 mutations per replication cycle. Drake also stipulated that the reasoning for this uniformity in mutational rate across diverse species had to have been evolved and was constant throughout species. As groundbreaking as this was for its time, as new technologies have arisen, we now know that not all organisms share a constant mutation rate of 0.0033, but some aspects of Drake’s rule still hold with regards to the relationship between genome size, effective population size, and mutation rates. More recent studies have been conducted using the various methods listed in this dissertation which can shed light on what was significantly harder to study during the time that Drake originally published his paper. Sung et al. revisits Drake’s publication and was able to generate data which

corroborates with the postulation that organisms have an inverse relationship between mutation rate and both genome size and effective population size. These findings can be seen in Figure 3.

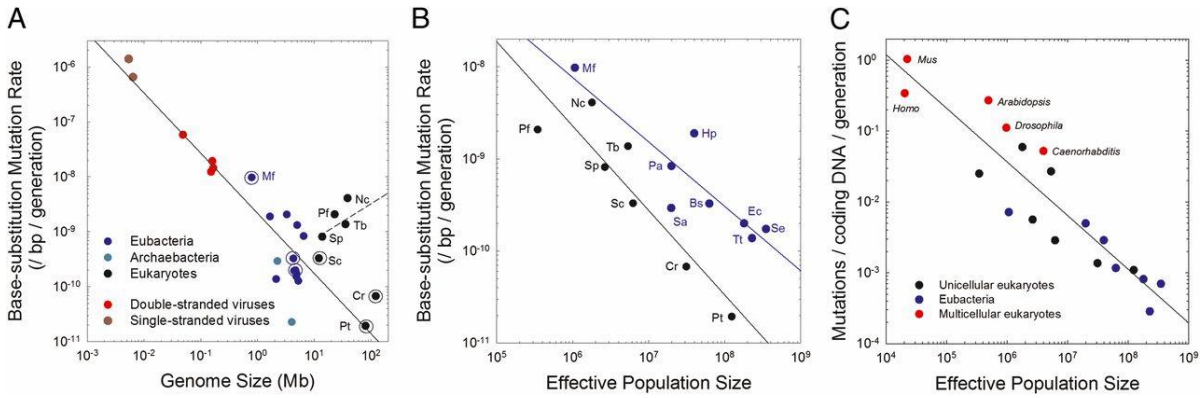

Figure 3. Produced by Sung et al. (A) Correlation between the genome size of various organisms and their base-substitution rate per site per cell division. (B) Relation between effective population size and base-substitution rate per site per cell division. (C) Relation between genome-wide mutation rate per cell division in coding DNA and effective population size.[57]

While their findings did show that mutational rates do vary between species, they demonstrate that there does seem to be an inverse relationship been both genome size and mutation rate as well as effective population size and mutation rate.

Drift Barrier

This work has revealed that mutation rates vary by over four orders of magnitude across the tree of life [58, 59]. Furthermore, this work has revealed that mutation rate evolution is limited by the drift barrier. The drift-barrier hypothesis is an alternative for Drake's rule and postulates that the lower limit of mutation rate that an organism can achieve is determined by its effective population size. An effective population of a species is defined as the total number or organisms within in a population that can contribute their genes to the next generation. These numbers vary greatly from species to species and in the case of bacteria can be upwards of 10^8-10^{10} [60]. The effective population is inversely proportional to the power of natural selection, therefore, the larger the effective population size, the stronger the ability for natural selection to refine and lower mutation rates. Under the drift barrier hypothesis, as a given trait is pushed towards perfection, any additional beneficial mutations (mutation rate reducin will have diminishing returns with regards to fitness. This means that at a certain threshold, it is unlikely that the effects of subsequent beneficial mutations will be significant enough to overcome the power of random genetic drift meaning, which will be $2N_es$ for haploid organisms and $4N_es$ for diploid [57].

Although the relationship between effective population size and mutation rates appear to be highly correlated, the organisms that have been assayed for mutation rates are limited to specific species [61] [57]. These species are easily bottlenecked on solid media, which makes them ideal candidates for laboratory experiments, but also means that they may not reflect natural populations very well. Clearly this shows a need for high-throughput mutation studies that can test these evolutionary hypotheses without these limitations.

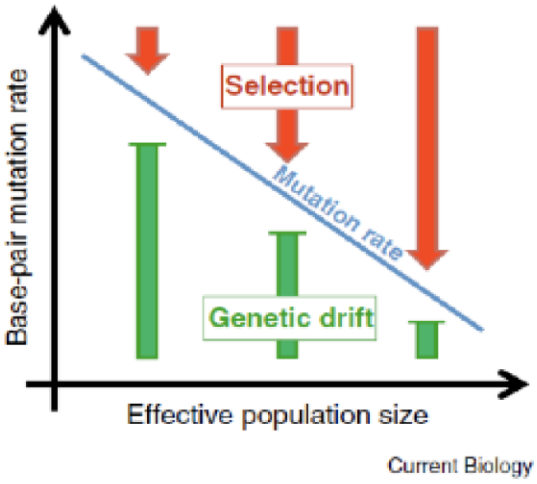

Figure 4: Genetic Drift versus Selection –As effective population size (Ne) increases, that fixation of mutations is driven less by genetic drift, increasingly by natural selection. Illustration by Sniegowski & Raynes from Current Biology 2013[62]

and

Chapter 2: Microfluidics, Applications, Background & Methods

Microfluidics

Microfluidics is a field that attempts to solve inherent experimental limitations by designing/implementing devices on a nano/micro scale which can be used to conduct experiments that were previously limited due to technology. In the context of biological experiments, these microfluidic devices can be used to accurately bottleneck cells in liquid media, perform automated tasks such as MA lines with the use of a pump system, or create isolated growth chambers. In a well-designed system, these assays can be used in real time while simultaneously conducting an experiment. In theory, experimental processes can be designed and implemented on chips should the need arise.

Another feature of microfluidic devices includes flexibility in design which can be utilized to address problems with current bulk cell studies. Thompson et al [26], produced a survey which lists the multitude of applications that microfluidic studies offer as well as their significant potential in expanding the field of single cell studies. Microfluidics offer the benefits of design flexibility, fluidic handling, thermal capabilities, automation, lower risk of contamination, as well as effective bottlenecking [26]. Given the flexibility in design, microfluidic setups can facilitate research well beyond the scope of single cell studies. Medical research can be conducted within a chip and used to study tumor cells, and their interactions with red and white blood cells [26].

Microfluidic studies on bacteria

Many scientists have been developing microfluidics to study evolutionary processes and population dynamics [2, 26, 63, 64]. Studies have been designed to bottleneck and isolate bacteria in different environments. For example, Robert et al. [2], were able to visualize the emergence of mutations within single cells of *E. coli* using a microfluidics device which they termed a mother machine [2]. They designed a microchip that was able to bottleneck and grow individual cells for over three days. Using imaging software, they tracked cells across 1000 microchannels in parallel, which produced roughly 200 generations in three days. They used the tracking to estimate fitness effects over 10^5 cells [2]. The device and experimental procedure are shown below.

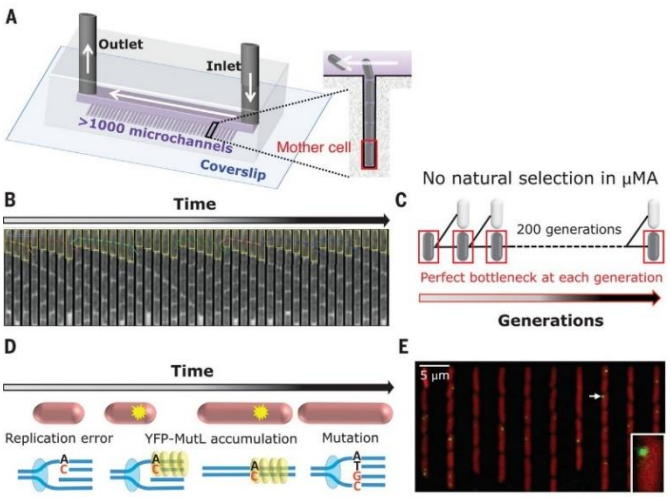

Figure 5. A "mother machine" microfluidic device used for bacterial growth. Diagrams B and C show bacterial growth overtime within this machine and the ability to maintain a single "mother" cell throughout the experiment. Diagram D and E are for tracking mutation sites [2]

This study showed the power of microfluidics in experimental evolution and mutation accumulation. Although this study succeeded in estimating mutation rates using a MA microchip there are a few issues with the design. First, trapping the organisms within single channels could lead to senescence (cell death), cell stress, or cell damage, that would influence mutation rates

and fitness measurements. Second, is that as cells replicate, they cut the previous cells off from the media, essentially starving the primary cells. Third, the cells are all pooled together making it difficult to determine the source, genomic location, and effect of the mutations.

Taxis

Microfluidics has also enabled research of bacterial taxis. These types of studies are relatively new as microfluidic technologies have become increasingly accessible and reproduceable and focus on bacteria motility under various conditions. These conditions can cover all aspects of environmental factors including temperature gradients and surrounding microenvironments which can provide information on all forms of motility through chemotaxis, thermotaxis, rheotaxis, magnetotaxis and phototaxis[65]. By better understanding the motile functions of various organisms, we can better understand design processes based on our experimental needs. For most bacteria, motility relies on self-propulsion using the bacterial flagellar motor (BFM). The BFM is a "reversible rotary nano-machine" powered by cation influx including H^+ and Na^+ and can also rotate at speeds upwards of 1000Hz[65, 66]. Bacteria have full control over their BFM and in instances of bacteria possessing multiple flagella such as *Escherichia coli* they are able to produce what is known as a "run and tumble" style of movement[65]. This "run and tumble" style of motility involves the switching between clockwise and counterclockwise rotation of the flagella during movement. By initially making

counterclockwise rotations, the flagella are tightly bundled up, generating a “run” motion. Once the “run” motion is finished, the flagella are then switched to clockwise rotations which transitions the bacteria into a “tumble” motion[65, 67, 68]. It is by combining these two styles of rotation that bacteria can orient themselves within an aqueous solution and swim towards their intended target. These motions can be seen in figure 5, as well as an enhanced image of the BFM.

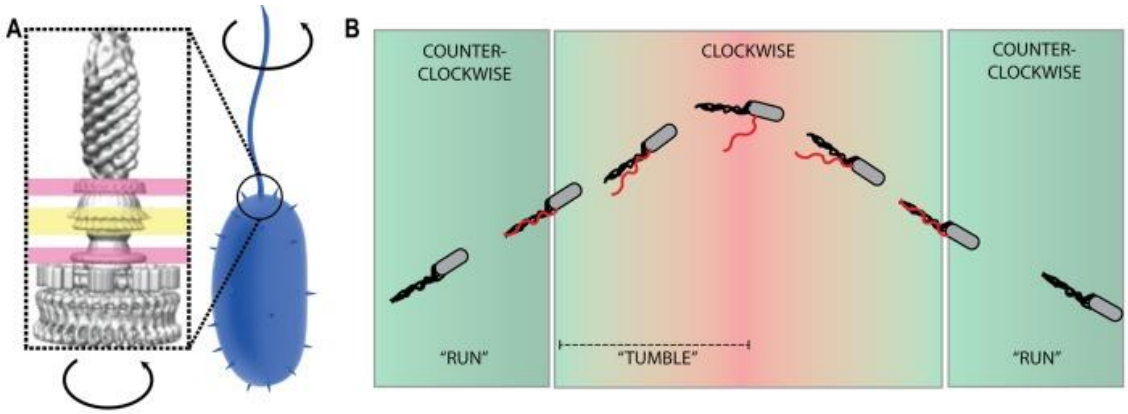

Figure 6. (A) Cryo-Electron microscopy tomography of the rotor of the flagellar motor structure. The inner membrane is highlighted in pink, and the peptidoglycan layer is highlighted in yellow. (B) “Run and tumble” motions of bacterial cells, counterclockwise rotations correspond to “run” motions and clockwise rotations corresponds to “tumble” motion.[65]

Having a better understanding of the nuances of microfluidics allows us to create more optimized designs. The behavioral study of bacteria within a microfluidic environment is still relatively new but with the increase in accessibility of 3D printing, as well as an increase in the performance of 3D printing machines, these studies are being performed more frequently. It is based on these studies as well as any new research that comes out that we chose to pursue 3D printing for our experimental process. Below, we will discuss the various methods and technologies used to fabricate 3D printed devices for various purposes.

Resin Materials

3D Printing (FFF printing)

Traditionally one of the most common forms of 3D printing, fused filament fabrication or FFF for short, is an accessible, user friendly method of printing objects. Most materials used for this method are safe, non-toxic, and many are biocompatible. One of the most common materials being polylactic acid (PLA), which is completely harmless to humans as well as biocompatible, which makes this an optimal material for biological experiments using FFF printing methods.

The general process of FFF printing involves a solid line of material being fed through a printer motor and up to a heated nozzle which then melts down the solid material into a gel-like form and extrudes it onto the print bed or printed object. The liquid material is then cooled and fused to the previous layers of the print job and re-solidified, creating a solid printed object. The nozzle on most printers can be exchanged for more specific openings ranging from 0.4-1mm, which controls the resolution of the print as well as the time it takes for the job to complete. The smaller the nozzle head opening, the more resolute the printed object will be, but it will also take exponentially longer to print.

Depending on the type of design and experiment required, there can be numerous shortcomings with this type of printing and material. When dealing with microfluidics there are issues with the highest resolution not being sufficient for functioning designs. This lack of resolution is more due to the process of FFF printing and material as the material is never truly water-tight unless heavily doctored post print. As PLA or most other materials re-solidify, very small gaps will form between print layers, which in the context of a microfluidics experiment will allow for leaks as well as places where individual bacteria can slip into and over grow or become lost.

Resin Printer (SLA printer)

Stereolithography printing (SLA printing) is an alternative and slightly less user-friendly form of printing but remedies the fundamental issues with FFF printing in terms of overall resolution and print quality. The materials used in SLA printers are always liquid resins which are toxic to touch although some are designed to be biocompatible, in the case of dental resins.

These resins are photo-sensitive and harden when hit with UV light. Most SLA printers involve a dark case to protect the liquid resin from light while a high-powered laser is shot through the print bed. As this laser scans over the print bed, it cures the resin one layer at a time and creates the solid printed object. Once the object is complete, it must be removed from the print bed and cured using isopropyl alcohol and cleaned thoroughly to remove any remnant liquid resin. Once cured in this manner it will need to soak in UV light for a duration of time to completely solidify the object.

The benefits of an SLA printer in the scope of a microfluidics experiments are that due to the nature of the printing process, a microfluidic chip will always be completely watertight as the resin is always solidified by the laser while being surrounded in liquid resin. The cost of these benefits come by increased print times as well as the extra caution that must be taken when handling the raw resin materials as well as post print treatments. However, with the rise of new technologies, overall print times have been drastically reduced allowing for comparable or even faster print times than traditional FFF printing.

3D model Creation

For any printing style, there are necessary steps that must be taken to generate a 3D mode. The initial steps involve the principal design of a desired object within some 3D modelling software called computer-aided design or CAD for short. The selected CAD software will allow the user to initially create 2D drawings of surfaces which will serve as the base for any

3-dimensional design. Once the user has generated a sufficient 2D schematic for the design, the next step in the process is called extrusion, which describes the process of converting a 2D drawing into a 3D space. This process can vary from software to software but in the general sense a plane or surface is selected, and then from that 2D space, parameters are specified as to how the extrusion is to proceed. Outside of physical impossibilities there is very little as far as limitations on what can be extruded and how. Once a 3D design has been created, a file must be generated and "sliced" into a format that is supported by a 3D printer. In order to generate these files, it is first required to export the file with an extension which can be read by the slicing software, which is most commonly an .STL file, which stands for stereolithography. Generally, this can be done by simply exporting your 3D object as the desired file extension, however, if an object is made up of numerous small parts combined together, then it is necessary to export all objects as a singular object. In the case of Solidworks, individual components are defined as parts, while a collection of parts placed together into a 3D object is called an assembly. Once an assembly has been created and uniformly exported as an .STL file, then it is ready to be read in by the slicing software. There are numerous slicing products available, and most 3D printers include their own proprietary brand. It is generally recommended to proceed with the slicing software that is paired with the specific 3D printer, in order to minimize printing issues.

Once a file is read into slicing software, various parameters can be specified by the user with regards to the printing instructions. These can include things like position of the object on the print bed, detection of any structural anomalies that could arise during the printing process, or generating support structures if the 3D object has any free-floating aspects which would fall apart or dislodge during the printing process. Once all options are specified and a print is ready to be created, then the slicing software "slices" the 3D model into a number of layers, which vary

depending on print resolution and dimensions of the object. These layers are then converted one by one into X, Y, and Z axis coordinates for the nozzle, or laser, depending on the model of the 3D printer, to follow during the printing process. These coordinates are saved into a file called the G code, which is essentially computer instructions for the printing process to follow. The printer will then start creating the 3D object one layer at a time, starting from the base of the object, and each layer will be built upon the previous layer. An example of what a typical slicing software looks like can be seen in figure 7.

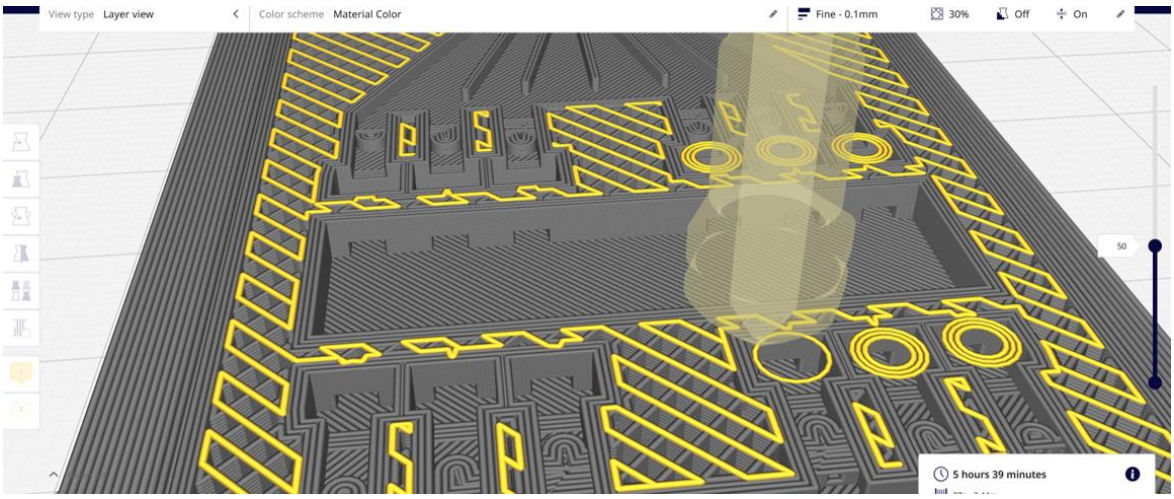

Figure 7. Slicing software preview for Ultimaker 3 FFF printer. The current layer being displayed is layer 50 of the 3D object and the path that the nozzle will follow for this layer is highlighted in yellow. All previous layers are grey as the model is built from the base up. Possible issues where support could be needed can be seen under the yellow circles as they are being printed over open reservoirs within the model.

Chapter 3: Concept and Design of Microfluidic Platforms for MA Experiment

MA experiments are an excellent way to determine the mutation rate of a given organism, however there are numerous shortcomings that are associated with these experiments. Some of these issues include the large amount of time required to generate colonies and produce an adequate number of generations in order to get the best calculation for mutational rates. Another key issue is that most bacteria cannot grow on solid media, which is problematic in that it is nearly impossible to limit the cell counts of bacteria in liquid media which they must grow in. We believe that it is possible to remove the limitations of solid media and optimize MA experiments while using liquid media. We propose the creation of a microfluidic device which can be used as a tool for optimizing MA experimentation studies. With this device, we will be able to produce multiple MA lines on a single chip, in a shorter time than would be possible using solid media, as well as use novel organisms previously impossible to study due to their liquid media restrictions.

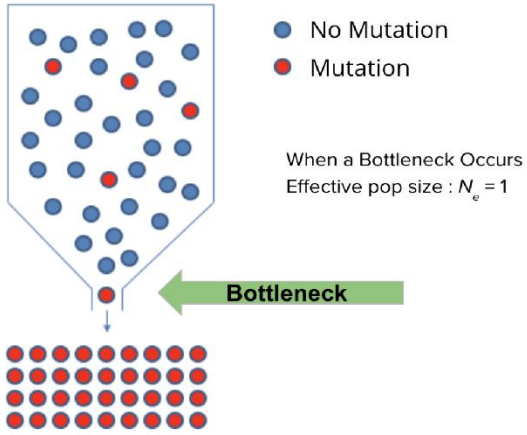

Figure 8: Bottlenecking – Illustration of the Bottlenecking process courtesy of the Sung Lab. When an organism is bottleneck occurs, the effective population (Ne) effectively becomes one. As a result, the fate of mutational fixation is entirely determined by genetic drift.

Microfluidics proof of concept and design.

The microfluidics project began with a simple design that had to meet specific criteria (Fig.9). The chip was to include multiple channels which could be continuously saturated with media to ensure numerous MA lines can be collected and grown simultaneously. Each channel would act as a unique and separate MA lineage which will allow for population bottlenecking as well as the accumulation of spontaneous mutations. Each chamber will have the ability to be individually seeded and as the cells replicate, continuous flow of media will ensure that all excess cells are flushed out of the channel and into the reservoir for collection. The collected cells will then be used for DNA extraction, library preparation, and Illumina high-throughput sequencing. Once sequenced, the mutation rates derived from the study will be contrasted to MA results of the same species grown in solid media from previous work. Additional chips will be constructed which will be highly customizable in order to research a wide range of pathogens and other bacteria, which are slow growing on solid media.

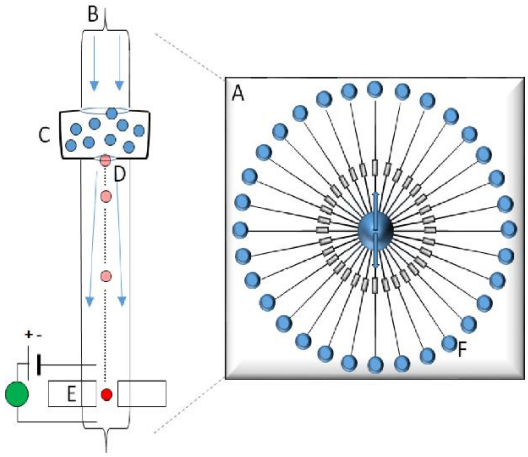

Figure 9: Prototype design: Proof of concept for microfluidics platform. Initially the platform was to be designed using a silicon-based organic polymer polydimethylsiloxane (PDMS). The design boasted an elevated reservoir in its center (Fig. 1A). The initial chamber would be seeded with cells (Fig. 1B). As the chamber fills with dividing cells (Fig. 1C), the flow of media will push the excess cells out of the chamber and into a reservoir (Fig. 5D). The initial concept also included a small on-chip micro-electrical system which could be used to count cells as they passed by (Fig. 1E).

Initial printing and issues

Initial chip designs were printed using the Ultimaker 3 FFF printer, which has one of the highest resolutions on the market compared to other FFF printers at the time, which was perfect for ensuring the highest possible accuracy for small prints. Our prints were performed using a 0.4mm nozzle head which defines the layer resolution, in this case it is 400 microns. The material we used in creating our devices is PLA which is completely biocompatible and easy to use. The total time it takes to create a chip ranged from 14-20 hours depending on the size of the device and number of channels on it. Once the chip was completed it was capable of use immediately as the material will have solidified and will be mostly sterile from being extruded at 210 degrees Celsius.

There were three major issues with the initial chip design. The most significant being the overall large cell counts, in that the actual number of cells being output from any given channel is far greater than what is expected, as shown by figure 5. This issue can be resolved by reducing the overall size of the chip and looking into alternative materials which can be used for printing.

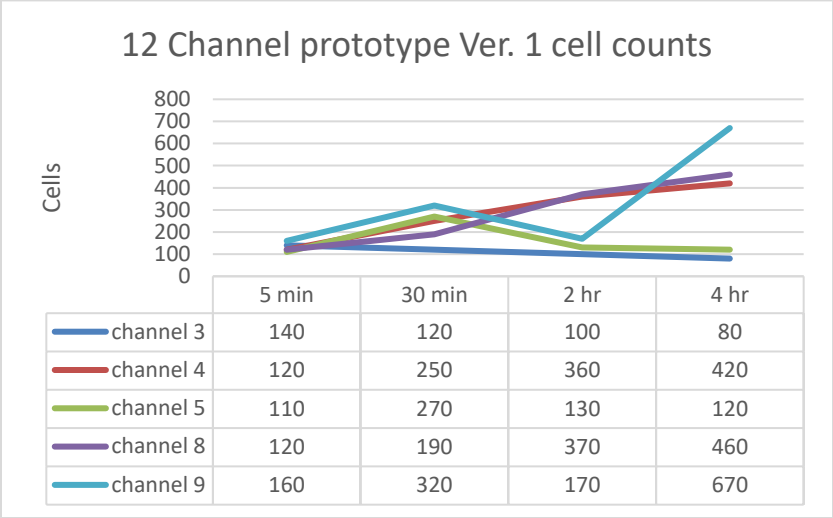

	5 min	30 min	2 hr	4 hr
channel 3	140	120	100	80
channel 4	120	250	360	420
channel 5	110	270	130	120
channel 8	120	190	370	460
channel 9	160	320	170	670

Figure 10. *Burkholderia* Initial cell counts performed on newly modified chip down to 12 channels from 24 channels. While overall cell counts have improved from hundreds of thousands of cells to only hundreds, there is still more reduction in count needed. Also, cell counts are not controlled well from channel to channel.

The second major issue with this prototype was the inability to reduce the overall size of the chip beyond a certain minimum. By reducing the size of the chip, we can effectively reduce the size of the bottleneck, thus reducing the overall cell count. This was difficult to accomplish as the resolution of the print is solely controlled by the size of the print nozzle, and as the nozzle becomes smaller, some of the smallest being 0.2mm, the prints begin to fail due to mechanical issues with the printer. When dealing with very small nozzles, it is common to see the melted resin fail to extrude from the nozzle and create a blockage, which will harden and render the print head useless. Once this occurs, it is extremely difficult to clean the nozzle out so that it may be used again.

The last problem with the FFF prints was that as the filament is extruded, it is poured on top of itself layer by layer, and as these layers harden there will be very tiny gaps which form

from the filament warping [69]. These tiny gaps within each layer provide a cavity for individual bacteria cells to occupy which can drastically throw off results. Any given channel within our chip can have countless cavities, ultimately creating multiple populations in each lane instead of our intended single population. This issue also contributes to the larger cell counts found in each channel and would produce highly variable cell counts from experiment to experiment depending on the number of cavities formed.

In order to correct for the issues of having a necessary print resolution smaller than the smallest setting on our FFF printer and the problems with the cavity formations during the printing process, we ultimately decided that we would have to modify the type of printer from FFF to SLA. This modification would solve nearly every issue that we have encountered with traditional FFF printing, and greatly increase the results of each experimental run.

Chapter 3.2: Prototyping, Refining, and Testing with MA Experiment

The primary function of our overall design is to ensure as many parallel MA experiment lines as possible while maintaining a proper bottleneck for our bacterial cells, while running for as long as possible with minimal human interaction. In order to accomplish this, we initially settled on a design which consisted of 24 total channels (12 on each side of the chip), but this led to numerous issues including flow rate issues which would prevent channels from being saturated with media during the experiment. The other issue that was created from this initial design was the number of output cells, numbering in the hundreds of thousands at a time when we are looking for as few as possible. This section will break down some of the cell counting performed, which allowed us to progress from chip version to newer versions, making small improvements with each change. The overall process is extremely time consuming from both a design and experimental perspective with a multitude of variables to consider. As each new version was tested, it would have to be run against all considerable variables such as flow rate, cell load, channel saturation, duration, and vacuum speed in order to ensure that all conditions were successfully being met before moving forward.

Identifying design error and prototype improvement

After the principal concept of the microfluidics chip was established, we moved into rapid prototyping and testing in order to ensure the design accomplishes our desired parameters. The prototyping process involved a great amount of time and methods in order to correctly test each design and find where improvements were needed. In order to develop our prototypes and make improvements we use Solidworks, which is a robust 3D modelling system that allows for the design of complex assemblies to be created as well as complex analysis to be run on any designed part. For the purpose of our experiment, we were able to perform fluid simulations and calculations in order to theoretically tell if the current chip will perform even before being printed.

Once a potentially successful chip file is printed, the chip then must be processed in order to remove any contaminates or liquid resin that has remained inside the chip during the printing process. This was done by soaking the newly printed chip in an isopropyl bath and flushing the core with pipettes. When this procedure was complete, the new chip was ready to begin testing, which initially begins with verifying that there are no print errors and that the flow rates of each channel match what was calculated within Solidworks. Flow rate is tested via a pump that is attached to each end of the chip and liquid is pumped into the chip at incrementally lower rates, until a baseline flowrate is established that can saturate all channels.

The second method we use for testing a successful chip is running the chip under the final experiment’s conditions and then performing cell counts for as long as possible. These cell

counts can be broken down further into two phases, the first being the overall cell count of the chip, and the second phase is to test for cross contamination from channel to channel. A successful chip will not only have as few cells as possible, but also only the channels that were initially loaded with cells will contain them during the counting process. While this experiment was conducted, it provided time for us to check for any external errors such as leaks or drainage issues that otherwise would not be observed.

The experimental process for initial cell counting involved the use of *Burkholderia cenocepacia.* Each horseshoe had a volume that had been calculated to hold around 50-100 cells of the bacteria being studied at the time. Our current version of the chip has horseshoes with dimensions of 0.39mm tall x 0.75mm wide, and either 1,2, or 3mm long, meaning each shoe has an estimated volume of either 0.29, 0.585 or 0.8775mm^3. It should be noted however that shrinkage can occur during the printing process which can range from a reduction in overall volumetric size from anywhere from 6 to 15 percent. This varies from printer to printer as well as from print to print so initial experimentation is required in order to accurately gauge the amount of volume that has been lost during the printing process.

Media was pumped into the chip at the pre-determined rate for as long as possible and cell counts will be performed regularly to monitor growth and contamination. As we migrated through various chip versions, we expected a drop in the overall cell count as well as increased length of runs. The data we have collected has indicated that this is the case, and each attempted improvement we have made has been accurate.

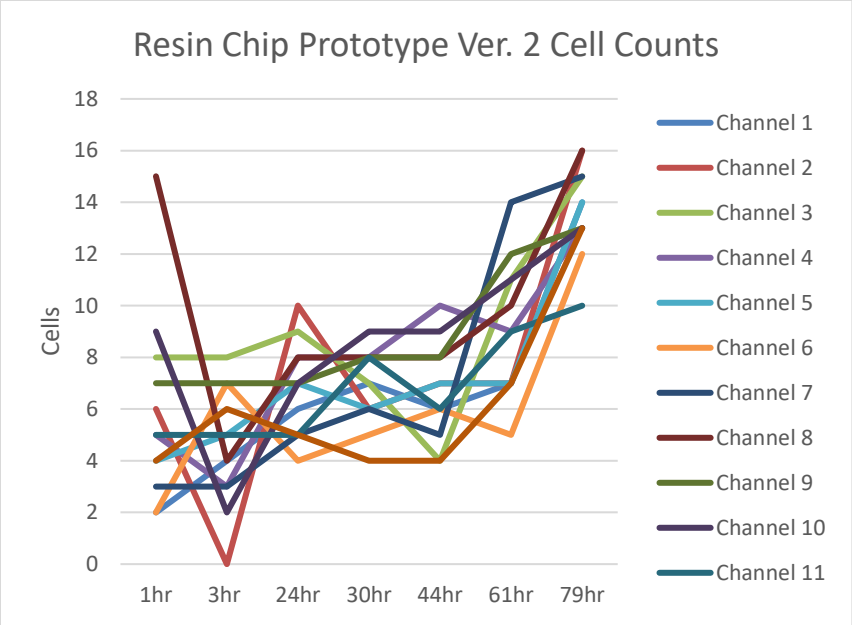

Figure 11 - *Burkholderia* Cell counts performed on chip design from Fig. 7. Overall cell counts are low, but consistency is an issue. There is also a contamination issue that consistently occurs around four to five days of running, which can be seen by the upward trend around the 79-hour mark.

The major issues we have encountered are mostly contamination. While we were able to consistently produce cell counts well within our expected range over time, overgrowth or foreign contaminations always happens. This can be due to multiple reasons. The first reason could be simply that *Burkholderia cenocepacia* produces a thick biofilm which eventually overtakes the chip core. The second issue could be breaks in flow throughout the chip which creates small pocket populations of bacteria which then get swept down the channels the next time media contacts it, creating increased cell counts. Additionally, there were also numerous uncontrollable factors which would ultimately lead to a run failing to complete. One of the most common issues with almost every version of our chip would be leaking from some critical point in the set up. Sometimes the tubing connecting the microfluidic chip to the pump would not create a perfect

seal and over the course of a five-day experiment would begin to leak media. Not only would this skew our cell counting but also drastically alter the overall flow and shear rates within the chip, leading to uncontrollable cell growth within a given side of the chip. As these leaks would surface, an experiment would have to be completely reset as the bottleneck of our cultures would be completely lost, meaning our cells were no longer under reduced selective pressure. The initial way we tried to combat leaking from the tubing was to simply warp para-film around the bast of the tube where it connected to the microfluidic chip. The idea would be that as media began to flow from the pump to the chip, and the vacuum pump started to pull from the chip, it would create a seal from the change in pressure should there be any small gaps between the tubing and entrance to the chip. This solution would work occasionally but it was not completely successful as leaks would still arise from time to time.

The next solution to this problem was to add the same liquid resin used to make the chip to the connecting area between the tubing and the chip entrance. The resin would then be placed under UV light to solidify the liquid resin, creating a perfect seal around the entrance. While this did solve our problems with leaking, it created different issues which affected the experimental runs. The first issue with this solution was that once the tubing had been sealed to the chip, there was no way to remove it without damaging the microfluidic chip. If any damage occurred, then an entirely new chip would have to be created to replace it.

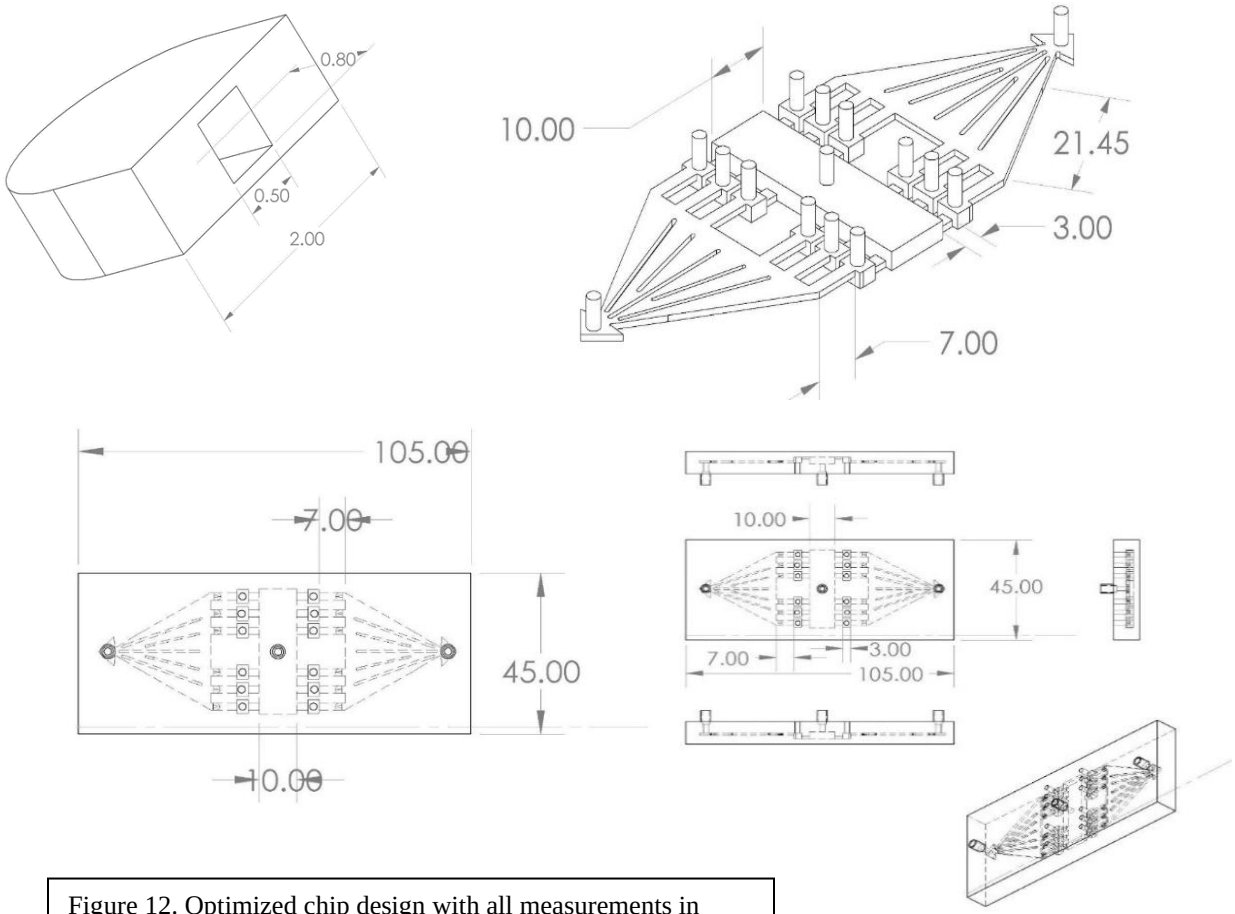

Figure 12. Optimized chip design with all measurements in mm. the horseshoe device serves as the bottleneck point and is embedded inside each channel, channel lengths are 7mm and horseshoes can range in length from 1mm to 4mm depending on needs.

Upon further study, it was determined that the majority of our contaminates arose from the bacteria's ability to swim upstream. Bacteria cells can attach themselves to an edge of each channel and swim upstream towards the entrances of the chip, ultimately contaminating the syringes which contain the media being pumped into the chip. It has been shown that certain bacteria are exceptionally good at swimming and will reorient themselves against flow whenever a small amount of flow is applied to them [70-72]. Another factor which adds additional complexity to this experiment is the fact that bacterial cells will swim differently depending on where they are located within a space, meaning closer to an edge, or existing on an upper or lower plane [70]. In order to help correct for this behavior, studies have suggested that a microfluidic chip must be designed in a manner such that flow rate can be maintained while maximizing shear rate on edges and other surfaces [71].

In these studies, shear rate is defined as:

$$V(y,z) = \sum_{nodd}^{\infty} \frac{4h^2 c}{\pi^3 n^3}[1 - \frac{cosh(\frac{n\pi y}{h})}{cosh(\frac{n\pi w}{2h})}]sin(\frac{n\pi z}{h})$$

Where c = $-(\frac{\nabla\rho}{\mu})$, μ being the dynamic viscosity and ρ being the pressure [71].

It has been suggested that replacing traditional rectangular channels with right handed screw patterns in conjuction with the above equation, one might be able to mitigate upward swimming and contamination within a microfluidic chip [71]. Our most current chip design follows this pattern and our data so far suggests that this is indeed the case. Cross contamination testing has been performed and the data collected can be seen in Fig. 7.

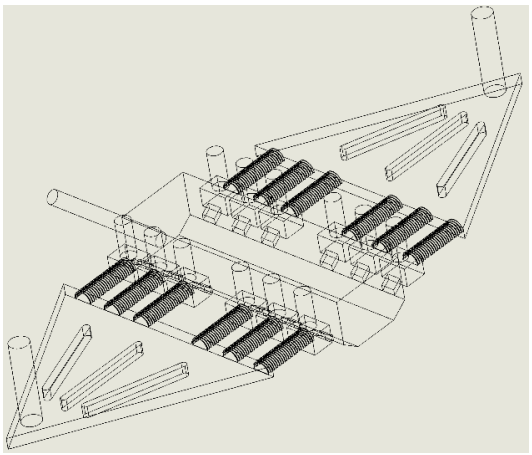

Figure 13. Most recent high-throughput version of chip with screw pattern channels. Overall design has also been optimized to ensure flow is always in the downward direction moving towards the central drain.

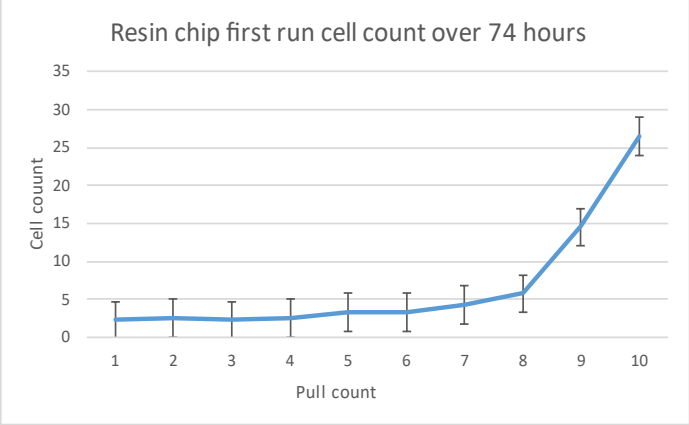

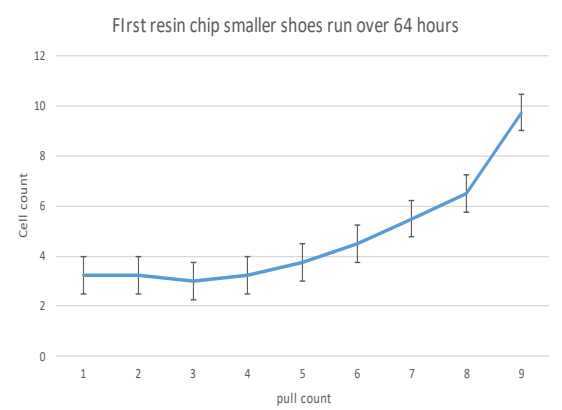

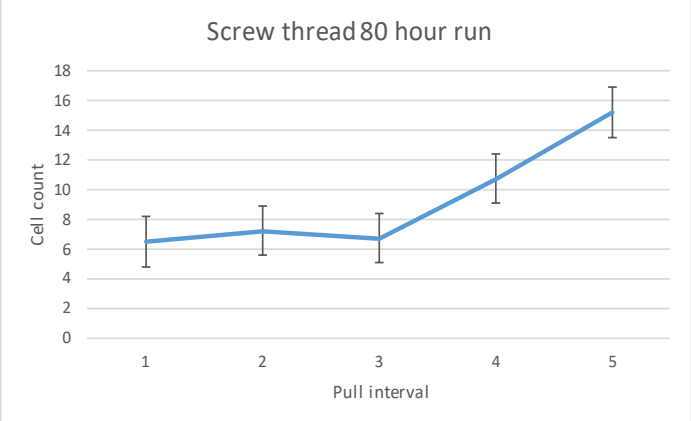

Figure 14. Channel cell counts of multiple attempted runs with newest chip. Top left was conducted 4 times, top right was conducted 4 times, and bottom left figure was conducted 4 times. Cell counts are averages of pull counts from the same channel over the course of the trial run.

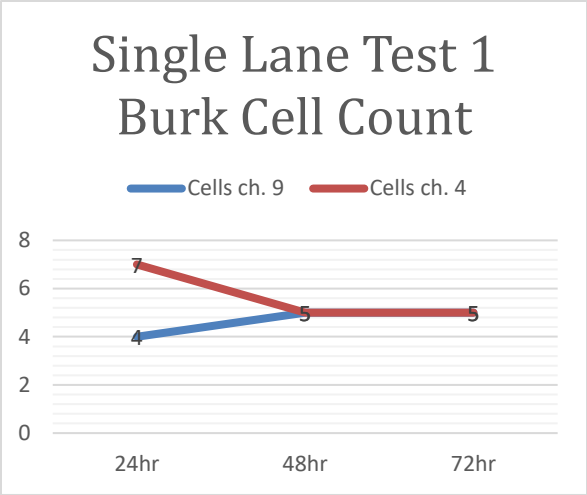

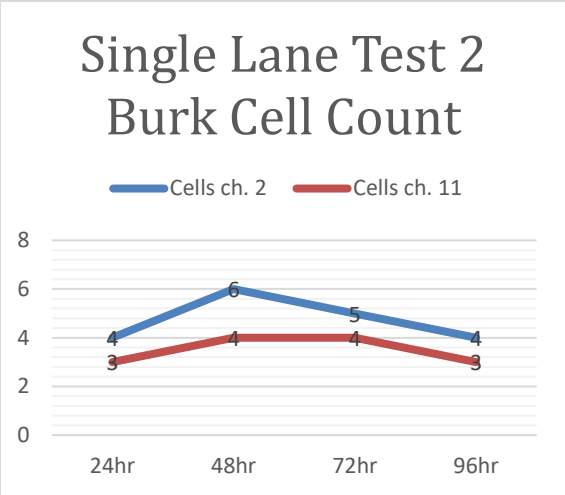

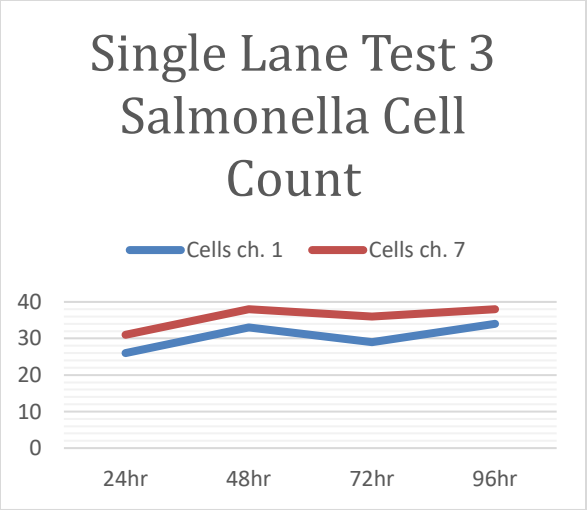

Figure 15. Cell counts conducted on individual channels on each side of the chip. Cells were collected and counted each day to monitor for cross contamination. In each graph, the only channels which contained cells were the ones initially loaded with cells. No cells were found in any of the remaining ten channels on each experiment. The third test was conducted using *Salmonella*.

The overall process of creating new versions of the microfluidic chip is quite challenging however, new and emerging studies are coming out which help gain insight on microfluidic experiments and methods in which we are able to optimize experimental design and procedure [73, 74]. Using these publications in addition to our own experimental data we are slowly moving towards a fully successful chip which can be implemented in a multitude of applications beyond the scope of this study.

Experimental run with *Salmonella* on Screw Thread Chip

The overall purpose of this experiment was to attempt to run a fully loaded microfluidic chip for as long as possible, while maintaining minimal cell growth as well as contamination. Initial set-up of experiment would only require the microfluidic chip to be loaded with bacteria and then attached to a pump via medical tubing. The loading process requires adding bacterial samples manually to each channel via the extraction opening using a 10μl pipette. As samples are loaded, saturation of horseshoe within the channel will be visually noticeable, and by adding the samples from the back of each channel, this prevents forward contamination into neighboring channels, which would be the case if loaded from the entry port. Once the microfluidic chip has been successfully primed, we attach it to our pump which is the “Harvard Apparatus PHD ULTRA” model microfluidic pump. This is an extremely precise, automated pump which provides flow accuracy within 0.25% and reproducibility within 0.05%. It has a dual pump system which allows for single or double syringe use and can hold syringe volumes ranging from

0.5µl to 140ml, and has a flow rate range between 0.0001µl/hr to 216ml/min. An additional peristaltic pump is attached to the drain tube and continuously runs through the course of the experiment to ensure that any media that has moved past the channels into the drain reservoir is promptly pulled out of the chip, minimizing the risk of overgrowth and contamination.

The parameters used followed our prototype testing protocol and the duration of this experiment was set for a total of 21 days of runtime. The minimal flow rate that would allow for complete chip saturation as well as maximized run time was 20µl/min. With two 100ml syringes at that rate, we can maintain a run for roughly 34 hours before having to refill the syringes with new media. This refill time is the only time where constant flow is broken and takes roughly 1 to 2 minutes depending on availability of replacement media. Knowing that this time could contribute to experimental errors including loss of cells, contamination, or backflow, precautions are taken to minimize those possibilities. Initially, separate medical tubes are used to refill each syringe, which ensures that the tubes connected to the microfluidic chip are never detached. These refill tubes are also kept in an isopropyl bath to ensure sterility. As syringes need to be refilled, the tubes are disconnected from the syringe end, and the refill tubes are attached, which is then used to draw in the replacement media. While this process is taking place, the peristaltic pump's pull rate is increased significantly in order to make up for the loss of flow. By doing this we better ensure the likelihood that any displaced cells are promptly pulled from the channel while maintaining enough force to continue containment of cells occupying the horseshoes. Once the media has been replaced, the tubes are reattached to the syringes and a short burst of a higher flow rate is performed as a "flushing" mechanic, which serves to rapidly re-saturate any channels

which might have had its media drained as well as wash out any cells which could be outside of the horseshoe device.

Over the course of this experiment, regular extraction of cells from select channels was done in order to perform cell counts. A volume of 10µl was extracted and placed on a hemocytometer for cell counting. Using the cell counts found in Fig. 9, we can identify any channels that have a higher cell count than expected, and then modify the run accordingly. Cell counts were performed within a window of 20-28 hours based on frequency of contamination or bacterial overgrowth that had previously been observed in earlier versions of the microfluidic chip. In addition to regular cell counting for quality control, samples would be extracted for each channel and stored to serve as a "checkpoint" should the current run fail and need to be restarted.

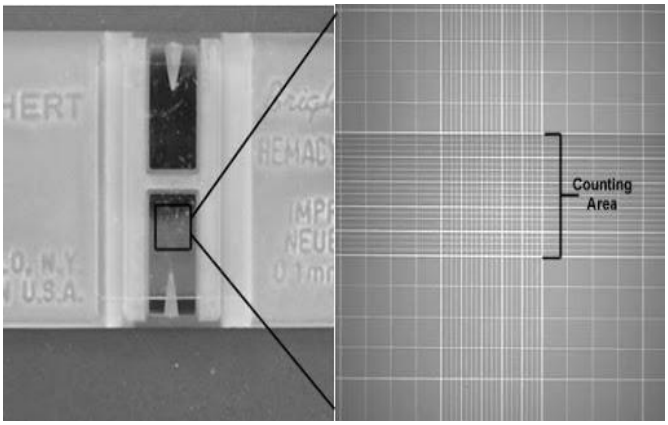

Figure 16. Hemocytometer used for cell counts. Magnified view of counting area on the right with varying levels of grid detail depending on the number of cells

Results

A total of two 21-day experiments were successfully conducted and a total of 48 samples were collected for sequencing and analysis. Two sets of twelve samples which were extracted after 21 days of being run through the chip, and two sets of twelve samples which were extracted on day 11 of each run. Once the experiments were concluded, the 48 samples were processed for sequencing using the Promega DNA extraction protocol. 1ml of overnight culture was added to 1.5ml microcentrifuge tubes and then centrifuged at 13,000 x g for 2 minutes. After, the supernatant was removed and 600µl of Nuclei Lysis Solutions was added. Cells were then incubated at 80 degrees Celsius for 5 minutes in order to lyse the cells. Once cooled to room temperature 3µl of RNase Solution was added to the cell lysate. We then incubated our cells at 37 degrees Celsius for roughly 30 minutes, and samples were cooled back to room temperature after. 200µl of Protein Precipitation Solution was added to the RNase treaded cell lysate and vortexed in order to mix the two solutions. Samples were then placed on ice for 5 minutes. After cooling, all DNA samples were centrifuged again at 13,000 x g for 3 minutes. The remaining supernatant was then transferred to a new container with 600µl of isopropanol. Containers were then inverted until visible strands of DNA form. DNA was then centrifuged again at 13,000 x g for 2 minutes in order to pellet the DNA samples. The Supernatant is removed, and 70% ethanol is added to the DNA in order to wash the pellet. After washing, the DNA is centrifuged at 13,000 x g for 2 minutes, and then the remaining liquid in each tube is drained and allowed to air dry for 15 minutes. Once dried, 100µl of DNA Rehydration Solution was added and then samples were

incubated at 65 degrees Celsius for 1 hour. Once this process was complete our samples were placed at 4 degrees Celsius for storage.

Genomic analysis

Genomes were globally aligned to our reference genome "NC_003197.2" using Samtools. The paired-end reads for each of our MA lines were individually mapped against the reference genome(assembly and annotation available from the National Center for Biotechnology Information, https://www.ncbi.nlm.nih.gov) using two separate alignment algorithms: BWA v0.7.4[75]. The resulting pileup files were converted to sam format using samtools v0.1.18[76]. Alignment information was further parsed to generate forward and reverse mapping information at each site, resulting in a configuration of 8 numbers for each line (A, a, C, c, G, g, T, t) and insertion deletion mutations, corresponding to the number of reads mapped at each genomic position in the reference sequence. Mutation calling was performed using a consensus method previously used in bacterial mutation analysis of many bacteria including *Burkholderia sp.*[57, 77-79]. This process involved the generation of new mutation calls by comparing the mpileup files of each sample against the reference file. These new mutation calls were then scanned on a per site basis, and confident calls were made based on the frequency of occurrence of each mutation across coverage per sample. This process was performed for both

SNP data and insertion and deletion mutations. Once these steps were completed, the files were generated for each type of mutation which contains the reference read, the chromosome, and nucleotide positions of each location that returned a mutation. These files were run against the GFF (general feature format) file and any known data about each position based on the genome was appended where appropriate. Functional Characterization of each mutation was achieved through NCBI(National Center for Biotechnology Information), and KEGG database[80]

Troubleshooting and optimization

Based on our data generated, it is evident that channel-to-channel contamination occurs during cell extraction. This was identified by the overwhelming number of shared mutations across lines within each sample group. There were also cases where an overwhelming portion of all mutations detected were within a single sample. Most of the mutations were INDEL mutations but ultimately the data was not of high enough quality for additional study. We had originally believed that the *Salmonella* samples we were provided with were miss-match repair deficient, which means the organism has no way to repair any mutations that arise during the experiment. After sequencing, we then realized that the miss-match repair gene was intact and present in our samples, which ultimately caused a significantly lower mutation count to work with than what was expected. In order to correct for this, additional microfluidic chips were

designed to eliminate the chance of channel-to-channel contamination at the cost of high-throughput functionality. While the high-throughput functionality of these new microfluidic chips is lost, they can be run for a significantly longer period, upwards of 144 hours before running out of media. These new designs feature the same protective measures designed in previous versions, with an additional layer of protection in the form of a thin wall diving the halves of the chip. This small division completely removes the possibility of either side of the microfluidic chip interacting with the other half.

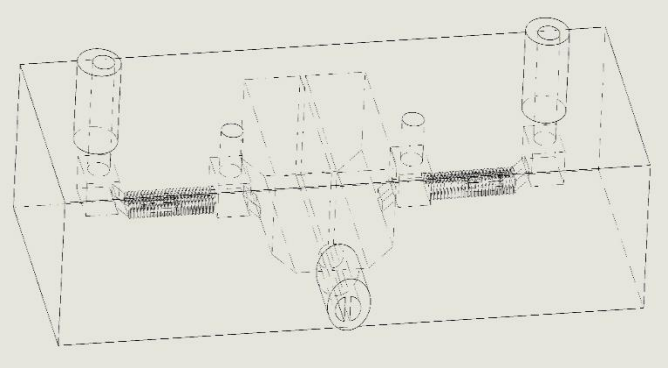

Figure 17. Single channel chip with division wall to prevent left and right halves from interacting, even after being drained from chip. Contains all modifications from previous designs.

Chapter 5: Collateral Sensitivity in *Burkholderia multivorans*

Introduction

The *Burkholderia cepacia* complex (Bcc) is a group of closely related Gram-negative bacterial species that are resistant to a broad range of antibiotics. Several Bcc species can cause chronic and debilitating lung infections in Cystic Fibrosis (CF) patients and presence of a Bcc species is usually associated with advanced lung disease[81, 82]. Once Bcc organisms have been established, the infection is usually chronic, and eradication is extremely difficult. Bcc is not generally found in pediatric patients, but approximately 3% of all CF patients are infected with Bcc organisms[83]. While prevalence is low, the risks associated with Bcc infections are high, including increased morbidity and mortality, and the potential for an often-fatal condition known as “cepacian syndrome” [81, 84].

Over the past decade the lifespan of individuals with CF has dramatically improved. According to the CF Foundation, the current life expectancy for CF patients born between 2017 and 2021 is 53 years, which is more than a 20 year increase since 2002 [84]. The recent development of CF transmembrane conductance regulator (CFTR) protein modulator drugs, has served to improve longevity and quality of life of CF patients [85]. Gene editing methods to correct DNA mutations within lung tissue could be a method to greatly reduce chronic bacterial lung infections in the future [86], but other infection treatment strategies are critical to supplement and combat ever-evolving bacterial infections.

Antimicrobial resistance is of particular concern in patients with CF [87], and no current antibiotic strategy is able to eliminate all target pathogens in the patient, creating an environment that provides time for the evolution of resistant mutants. Many genes involved in antibiotic resistance are observed to evolve within CF patient studies, such as upregulation or deregulation of efflux pumps [88] and mutations in stress tolerance regulatory components [89]. Multi-drug resistance (MDR) and cross-resistant strains have become a problem not only in CF patients and Bcc, but also many other infectious bacteria.

When a bacterium evolves resistance to an antibiotic, it can often become susceptible to a non-treatment antibiotic for which the bacterium has not been exposed. That response is called collateral sensitivity (Fig. 18) [89-91]. Collateral sensitivity interactions between two antibiotics can be either reciprocal, whereby direct resistance to either drug in a pair leads to an increase in sensitivity to the other, or asymmetrical, in which direct resistance to Drug A leads to an increase in sensitivity to Drug B but the reverse does not occur [91, 92]. Identification of collaterally sensitive (CS) antibiotic pairs has the potential to form the basis for long-term treatment of chronic infections by limiting life-long therapy to switching between two members of a reciprocal CS antibiotic pair – when resistance to one member of the pair occurs, the patient is switched to the other member of the pair; when resistance is acquired to that second antibiotic (resulting in loss of resistance to the first antibiotic), the patient is switched back to the original drug.

In this study, we plan to identify candidate genes that are involved in collateral sensitivity to antibiotics. Here, we expose multiple lineages of a clinical strain of *Burkholderia multivorans* to various antibiotic treatment regiments in order to evolve collateral sensitivity and resistance. Mutations that arise repeatedly during sensitivity are primary targets for collateral sensitivity and

can be used as an informative genetic screen for drug sensitivity. Once identified, we can expand on the knowledge of mutational effects of drug sensitivities and better demonstrate the interactions between genes that contribute to varying drug resistances and sensitivities.

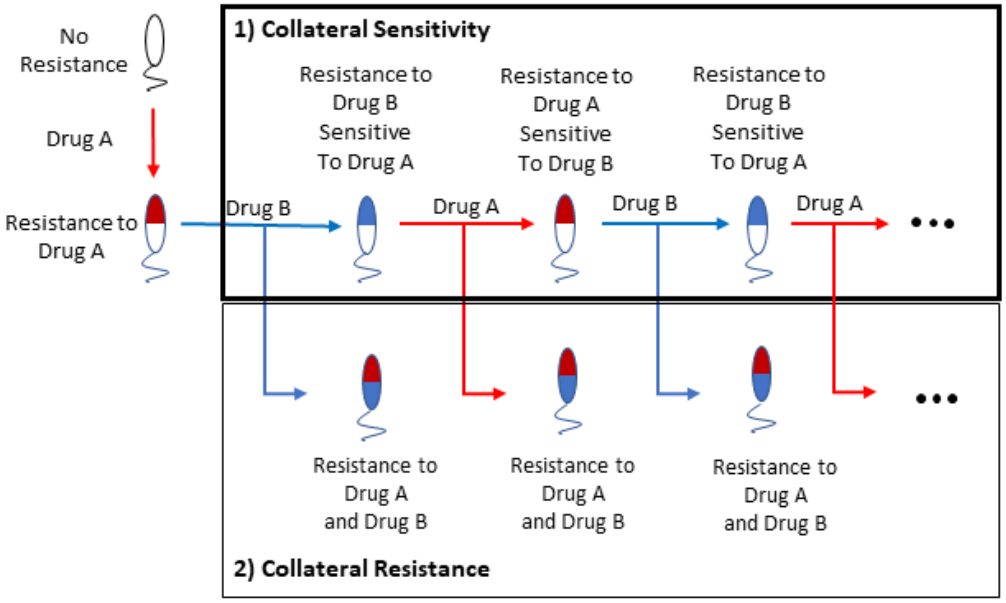

Figure 18. Collateral Sensitivity**:** A given bacteria cell with no known resistances or sensitivities is introduced to drug A. After developing resistance to drug A, it is then introduced to drug B. 1) demonstration of collateral sensitivity where the development of resistance to one type of drug produces a sensitivity development to another drug. 2) Collateral resistance is the alternative to collateral sensitivity, where a given bacteria maintains its principal resistance to drug A and develops an additional resistance to drug B.

Material and Methods

Collateral sensitivity (CS) occurs when a strain that acquires resistance to one antibiotic simultaneously exhibits increased sensitivity to a second antibiotic. This is detected experimentally by exposing cells to one antibiotic (the treatment drug [TD]) and then, when resistance is acquired, assessing for a change in minimum inhibitory concentration (MIC) to antibiotics that strain was not exposed to (i.e., non-treatment drugs [non-TD]). We used antibiotic discs and zone-of-inhibitions (using Clinical and Laboratory Standards Institute [CLSI] breakpoints) to designate strain resistance, and ETEST® to quantify MIC. An increase in MIC to a non-TD reflects collateral resistance (CR); a decrease reflects CS.

Each *B. multivorans and B. cenocepacia* strain was evolved for resistance to each of six antibiotics (the treatment drug [TD]), then screened for change in MIC towards the other five antibiotics (the non-treatment drugs [NTD]). Strains exhibiting increased sensitivity towards any NTD (i.e., exhibit collateral sensitivity [CS]) were then evolved to resistance towards that NTD (i.e., the NTD becomes the TD). Once resistance to the new TD was acquired, the strain was screened for change in MIC towards each NTD. Reciprocal CS occurs when resistance to antibiotic A occurs simultaneously with sensitivity to antibiotic B, it simultaneously becomes sensitive to antibiotic A.

Strains, culture conditions, and antibiotics

Species and strains included in this study were chosen based on consultation with Dr. John LiPuma, are naturally competent, and have an existing reference strain for sequence analysis. Bacteria was grown at 37˚ in ambient air on LB broth for routine culturing and during experimental evolution. Mueller-Hinton broth 2 plates were used for antimicrobial susceptibility testing.

The six antibiotics involved in this study (chloramphenicol, ceftazidime, levofloxacin, meropenem, minocycline and trimethoprim/sulfamethoxazole) were chosen based on being commonly prescribed in the U.S. for treatment of CF patients, having a varied mode of action, and able to be tested using ETEST® strips. Although some of these antibiotics are used in combination with a beta-lactamase inhibitor (e.g., piperacillin/tazobactam), this project was focused on collateral-sensitivity to the antibiotic.

Experimental Evolution

Burkholderia strains were evolved for resistance to each treatment drug (TD). In brief, each strain was swabbed onto LB agar to create a lawn, then an antimicrobial susceptibility test disk was added to the center. After 16-24 hours incubation at 37˚C, the growth closest to the zone of inhibition was collected and used to inoculate the next plate until resistance was achieved. Strain evolution was stopped when antimicrobial susceptibility testing via disk diffusion on Mueller-Hinton agar plates exhibited a zone of inhibition (ZOI) that is considered

‘resistant’ by the CLSI breakpoint or there is growth up to the disk for the antibiotics that do not have a disk diffusion breakpoint (e.g., LVX).

Antimicrobial susceptibility testing and interpretation to identify collateral sensitivity.

Disk diffusion testing was performed on strains selected for resistance to a treatment drug (TD) to determine susceptibility to each non-TD antibiotic. Disk diffusion to the TD was examined to ensure the strain is resistant, and not due to plating or growth issues [93]. The antibiogram of the evolved strain was compared to the antibiogram of the parental strain. A change in ZOI of 20% or greater for a non-TD reflects a collateral change in susceptibility; an increase in ZOI indicates collateral sensitivity (CS), a decrease in ZOI indicates collateral resistance (CR) [94]. Finally, an ETEST® was used to determine the minimum inhibitory concentration (MIC) on all strains having CS based upon the disk diffusion assay. A decrease in MIC from the ETEST® indicates increased sensitivity, allowing us to confirm that collateral susceptibility has arisen.

Whole-genome sequencing

Whole-genome sequencing of each lineage when CS was detected was performed at the University of New Hampshire using 250 bp paired end reads with an Illumina HiSeq 2500 platform.

Genomic analysis

Genomes were globally aligned to a reference genome using Samtools. The paired-end reads for each MA line were individually mapped against the reference genome (assembly and annotation available from the National Center for Biotechnology Information, https://www.ncbi.nlm.nih.gov) using two separate alignment algorithms: BWA v0.7.4 [75]. The resulting pileup files were converted to sam format using samtools v0.1.18 [75]. Alignment information was further parsed using mpileup files to generate forward and reverse mapping information at each site, resulting in a configuration of 8 numbers for each line (A, a, C, c, G, g, T, t) and insertion deletion mutations, corresponding to the number of reads mapped at each genomic position in the reference sequence. Mutation calling was performed using a consensus method previously used in bacterial mutation analysis of many bacteria including *Burkholderia sp*[57, 77, 78, 95, 96]. Functional characterization of each mutation was achieved through NCBI (National Center for Biotechnology Information) , Burkholderia Database (Burkholderia.com), and KEGG database [80].

Mutation Analysis

Once sequence data was processed, we generated our mutation data via a series of perl and bash scripts. This process involved the generation of new mutation calls by comparing the mpileup files of each sample against the reference file. These new mutation calls were then

scanned on a per site basis, and confident calls were made based on the frequency of occurrence of each mutation across coverage per sample. This process was performed for both SNP data and insertion and deletion mutations. Once these steps were completed, the files were generated for each type of mutation which contains the reference read, the chromosome, and nucleotide positions of each location that returned a mutation. These files were run against the GFF (general feature format) file and any known data about each position based on the genome was appended where appropriate. Completed and annotated files were then grouped based on lineage and compared to each other to generate a consensus file for each lineage. This process was repeated across lines, including the parental line of each sub-lineage in order to detect shared mutations that could have appeared across lines.

Results

Identification of collateral sensitivity in B. multivorans

Using a *B. multivorans* isolate from a 30-yr-old male cystic fibrosis patient, a total of 279 strains were evolved to be resistant to six treatment antibiotics (chloramphenicol [CHL], ceftazidime [CAZ], meropenem [MEM], minocycline [MIN], levofloxacin [LVX], trimethoprim-sulfamethoxazole [SXT]). Two of these six antibiotics are beta-lactams (βLA) [CAZ, MEM], and four are not (non-βLA) [CHL, MIN, LVX, SXT].

Collateral sensitivity (CS), cross resistance (CR), and the patterns for strains exhibiting both CR and CS were described. Of the 279 evolved strains, 188 (67%) exhibited cross-resistance and 170 (61%) exhibited collateral sensitivity. The frequency for each of the six

antibiotics is seen in Table 3. The range of cross-resistance frequency for each treatment drug varied from 58% (meropenem) to 90% (chloramphenicol). The range of collateral sensitivity frequencies ranged from 56% (ceftazidime and minocycline) to 70% (trimethoprim-sulfamethoxazole).

Of the 170 strains that exhibited collateral sensitivity, whole genome sequencing and mutational analysis was applied to 48 of the strains (Fig. 19). The parental strain (149) was also sequenced. Outside of the parental strain, we observed a total of 555 mutations across these lineages, dominated by insertion-deletion mutations (indels, 92.8%). Almost half of the mutations (45.8%) were found in coding regions and the high number of indel mutations ensured that a majority of the mutations (98.0%) led to nonsynonymous changes and premature stop codons.

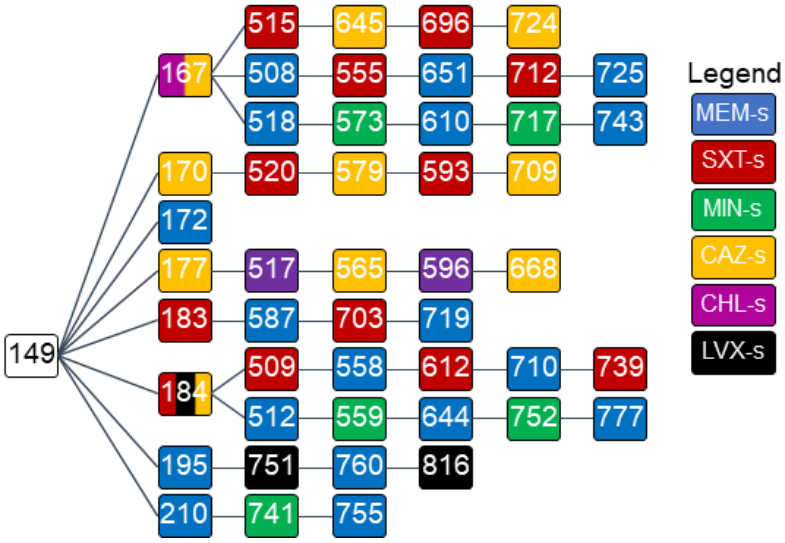

Figure 19. Visualization of *Burkholderia* lineages colored based on their drug sensitivity. Alternating patterns of sensitivity development can be seen, indicating the "flipping" nature of parent to child drug sensitivities.

Lineage	#	Snps	Indels	Flips	P.Flip	Syn	NonSyn	Total
	8	9	79	NA	NA	2	40	88
167-555	5	2	47	47	2	1	12	49
167-518	6	5	57	61	1	1	12	62
167-515	6	1	49	45	5	1	22	50
170	5	4	51	49	6	0	23	55
172	1	1	25	NA	NA	0	11	26
177	5	3	41	41	3	0	25	44
183	4	1	86	77	10	0	44	87
184-509	6	7	28	32	3	0	18	35
184-512	6	10	33	43	0	1	27	43
195	4	0	63	59	4	0	31	63
210	3	6	35	NA	NA	1	24	41
Total	51	40	515	454	34	5	249	555

Table 3**.** summary of mutation information sectioned by lineage, total number of mutations can be seen as well as the spectrum of mutation types, and frequency of flipping mutations and perfectly flipping mutations.

Mutations that arose when a strain evolved antibiotic sensitivity and reverted during antibiotic resistance were identified as a "flipper" (Flippers, Fig. 19). "Perfect flippers" (P. Flip, Table 4), indicated that the mutation arose and then reverted perfectly with respect to the sensitivity and resistance. An example of a "perfect flipper", can be found in lineage 170 at position 1538652, which was first observed when the strain evolved CAZ-sensitivity (strain 170). The strain was evolved to be resistant to CAZ and sensitive to SXT (strain 520), and after sequencing revealed the mutation reverted (strain 520). The strain was then evolved to be

resistant to SXT and sensitive to CAZ (strain 579), and the indel was again observed. This cycle where the indel was observed during CAZ sensitivity and reverted during CAZ resistance repeated for two more evolutions (strain 593 and strain 709). These perfect flippers are ideal candidates for combating antibiotic resistant strains using gene therapy.

Across the lineages, collateral sensitivity was observed in many different combinations. We looked across all resistances and sensitivities for recurrent mutations that arose more than once in different lineages. These mutations were not exclusive to the lineages or sensitivities where they arose, and most of them were present regardless of the specific antibiotic sensitivity. The breakdown of mutations across all samples based on antibiotic sensitivity can be seen in the table below.

	CAZ-s	SXT-s	CHL-s	MEM-s	LVX-s	MIN-s
CAZ-s	66%	49%	64%	72%	64%	82%
SXT-s	40%	55%	51%	46%	16%	56%
CHL-s	31%	51%	100%	41%	50%	50%
MEM-s	51%	49%	58%	57%	27%	65%
LVX-s	0%	0%	0%	0%	0%	0%
MIN-s	0%	0%	0%	0%	0%	0%

Table 4**.** number of occurring mutations from “true flipper” positions across all samples grouped by antibiotic sensitivity. Left column indicates sensitive group where “true flipper” arose, and the frequency of mutations across all sensitive groupings. There were no “true flipper” mutations that arose in LVX-s or MIN-s lines.

Discussion

In our work, we have evolved sensitivity multiple times across different lineages and using different antibiotics. Here, we discuss the mutations that are associated with the lineage where collateral sensitivity arose and in the scope of the antibiotic that was applied. All these mutations were insertion-deletion mutations which dominated the mutations within the lineages.

Antibiotics, Mechanisms of Action and Perfect Flippers

Antibiotics

In the following section, we will discuss the 6 antibiotics used in this study (Meropenem, Minocycline, Levofloxacin, Chloramphenicol, Sulfamethoxazole/Trimethoprim, and Ceftazidime) and their mechanisms of action as they pertain to antibiotic resistance and sensitivity.

The function of Meropenem (MEM) is to prevent the formation of the bacterial cell wall via binding to and inactivating the penicillin-binding proteins [97]. There are a few reasons for MEM resistance to arise in bacteria, mostly focused on the ability to prevent MEM from reaching penicillin-binding proteins. This can be achieved by a diminished expression or loss of

porin proteins reducing the permeability of the cell, and preventing MEM from ever entering [97]. Another mechanism for resistance could be an increase in expression in efflux pumps which are used to expel MEM from the cell once it has entered the periplasmic space and can ultimately lead to multidrug resistance [97].

Second, Minocycline (MIN) is a drug within the tetracycline family that acts as an inhibitor of bacterial protein translation. MIN will bind to the helical region of bacterial ribosomes, blocking the incorporation of amino acids into peptide chains, greatly preventing formation and growth [98].

We identified perfect flippers within the TetR family transcriptional regulators and efflux pump genes in strains sensitive to MIN. Efflux transporters are responsible for secreting toxic material including antibiotic drugs. Efflux pump alterations within the drug's target sites have been shown to be associated with antibacterial resistance to tetracyclines [98].

Third, Levofloxacin (LVX) is a quinolone with three recognized mechanisms of resistances: mutations that alter antibiotic target sites, plasmid mediated protection which reduces the overall effect of the antibiotic, and mutations that cause reductions in antibiotic accumulation such as efflux pumps and cell permeability [99]. By changing gene expression, gram-negative bacteria are able to alter permeability through porin proteins which form channels for passive diffusion [99]. Perfect flipping was observed in mutations for Porin and efflux transporter outer membrane subunit proteins in strains sensitive to LVX.

Like the antibiotics mentioned above, Chloramphenicol (CHL) alters the targets of medication, efflux and pump systems that can mediate the flow of molecules within and through a cell, and horizontal conference of resistance can all contribute to CHL resistance in bacteria

[100]. Indel mutations within the gene for the putative multidrug efflux transcriptional regulator *CeoR* were found within strains resistant to CHL.

Sulfamethoxazole/trimethoprim (SXT) is a combined antibiotic composed of five parts sulfamethoxazole and one part trimethoprim. Sulfamethoxazole functions by directly targeting the synthesis of folate in bacteria. It works by inhibiting the activity of dihydropteroate synthase enzymes and competes with p-aminobenzoic acid (PABA) during the formation of dihydrofolate [101]. When used together with trimethoprim, an antibiotic that stops the conversion of tetrahydrofolate, the combination disturbs the synthesis of purines, thymidine, and methionine that are essential to produce DNA and proteins in bacterial replication. The purpose of this combination is to cause a bacteriostatic halt of replication. While there were a number of mutations found in SXT-sensitive lineages, no perfect flippers were found.

Ceftazidime is an antibiotic belonging to the drug class, cephalosporins. Similar to other beta-lactam antibiotics known resistance mechanisms include the expression of beta-lactamase enzymes, altered drug targets such as conformational changes in penicillin-binding proteins (PBPs), reduced bacterial permeability, and increased drug efflux via efflux transporter outer membrane subunit [102].

Perfect flippers

We identified perfect flippers in multiple genes that are known to be involved in resistance traits. First, we observed a mutation in Virulence protein E, which is a protein family that determines how well a organism can infect a host and cause disease [103]. Factors driving virulence are generally involved in secretory, membrane associated, or cytosolic [103] and allow bacteria to respond differently to targeted antibiotics that attempt to reduce their overall virulence [104].

Second, we identified a perfect flipper in chloride channel proteins, a family of channel-like protein structures that play a vital role in a number of cellular functions across all types of organisms. Some of these functions include regulatory processes which help control the state of the ionic composition of the cytoplasm, as well as cellular volume in tandem with other pump systems [105].

Third, we identified a perfect flipper in an anti-sigma factor gene which is the antagonist to the sigma factor responsible for regulating gene transcription [106]. There is a very wide range of cellular processes that can be regulated by anti-sigma factor, which include growth, flagellar biosynthesis, ion transport and virulence [106].

Multiple mutations were identified as perfect flippers in CAZ-sensitive lines. First, we observed an indel mutation in Chemoreceptor glutamine deamidase *CheD*, which is responsible for the deamination of chemoreceptors. *CheD* plays a critical role in the ability and functionality of chemotaxis of an organism [107], and inhibition prevents an organism's ability to detect and

respond to changes in chemistry within its environment. This means that a bacteria will no longer be able to detect nearby concentrations of nutrients or increasing concentrations of toxins such as antibiotics and relocate itself accordingly [107]. Our results indicate that *CheD* plays a role in numerous antibiotic sensitivities, including MIN, MEM, and SXT. However, the strongest indication is with CAZ sensitivity, where we see 'true flipping' of mutations through the lineage that are sensitive to this antibiotic, alternating from parent to child strains.

Second, we identified a flipper mutation in DNA ligase D, an enzyme that is critical to the repair of lethal double-stranded breaks in bacteria [108]. DNA ligase D is part of the nonhomologous end-joining pathway, which is an alternative repair method from homologous recombination [108] and can ultimately bind and repair gaps formed from these breaks [108, 109]. Any loss of functionality of this enzyme would prevent a bacteria's ability to repair critical DNA errors which arise from double-stranded breaks and may prove fatal to the organism. Based on our sequencing analysis, DNA ligase D seems to have a significant role in CAZ sensitivity based on its 'true flipping' across a line and could play a minor role in other sensitivities to MEM and MIN antibiotics.

Third, we found a mutation in the BON domain-containing protein is part of a domain that has a direct relationship to the permeability of the cell membrane [110]. The loss of this gene would increase the fluidity of the cell membrane which would significantly decrease the bacteria's ability to protect itself from detergents and antibiotics [110]. The only antibiotics that seem to be affected by a mutation in this gene in our study are in a small part MEM, and CAZ. Samples that had alternating CAZ sensitivities were the only ones to possess 'true flipping' mutations within the BON gene.

Our fourth perfect flipping mutation was found in Nodulation protein *NfeD*. This protein structure is present in almost 300 bacterial and archaeal genomes, and is believed to have a role in the quality control of select membrane proteins [111]. With regards to antibacterial resistance, there is little research to be found outside of certain plant bacteria, where *NfeD* proteins help with the bacterial infection of host roots [111]. It's perfect flipping nature in our samples which flipped between MEM and SXT sensitivity make it an ideal candidate for further research.

Finally, we identified a perfect flipper in Flavin reductase which is an enzyme that has an important biological role involving the catalyzation of flavin reduction through NAD(P)H oxidation [112]. There are several flavin reductase proteins that vary from organism to organism. It has been reported that a particular family of bacterial flavin reductase proteins plays a significant role as an electron transport mediator [112]. There was only one instance in our results that indicates a critical role in antibiotic sensitivity within a lineage, and that was CAZ sensitive lines.

In addition, to perfect flippers, there were a significant number of mutations (flippers) that could contribute to the evolution of collateral sensitivity. Many of these flipper mutations were in genes that are also known candidates for antibacterial resistances such as porins, which serve an important role in gram-negative bacteria, due to these bacteria having a thin outer membrane that functions as an additional protective barrier, toxic chemicals, including antibiotics, are inhibited from entering the cell. Porins specifically are outer membrane proteins that are associated with the modulation of cellular permeability and antibiotic resistance [113]. penicillin binding proteins, which are enzymes involved in the assembly of the bacterial cell wall serving as a major target for antibiotics. Specifically, these enzymes work by binding to penicillin and other beta-lactamase antibiotics, a necessary process for bacterial cell wall

synthesis or biosynthesis [114]. and efflux transport outer membrane subunits [113-115]. These subunits are made up of energy-transducing inner membrane subunits and the conduit outer membrane subunits. Harmful substances that are secreted into the environment, such as antibiotic medications, are released by efflux transporter outer membrane subunits, and are readily used by many gram-negative bacteria, these pumps confer modest resistance to clinically important antibiotics while more complex resistance mechanisms may emerge [115].

In combination, these effects can greatly impact antibiotic resistance. Lastly, we find that five perfect flippers were found in hypothetical proteins which are unannotated genes. These genes are candidates for study as unknown proteins that can interact or create sensitivity for different antibiotics.

Conclusion

Having gained a better understanding of the interacting effects of mutations and how they assist in driving collateral sensitivity, we can use this information to gain insights on candidate genes which have a significant impact on drug resistance and sensitivity. By studying these mutations and the loci in which they arose, targeted gene editing may be feasible to induce antibiotic sensitivity and help ensure that an infection can be effectively cured without the potential for new strains of resistant bacteria to arise. Successful gene editing can also alleviate some of the costs and pressures of having to stack medications or administer alternating medications in order to maintain treatment efficiency as bacteria gain resistance to traditional antibiotics. More research needs to be done but hopefully this study provides an alternate

pathway for standard methods of dealing with bacteria which are multi drug resistant or have the ability to rapidly gain resistance.

Mutations that gave rise to perfect flippers were present only within a given lineage and not found in other lineages that shared the same sensitivity. We identified zero instances where perfect flippers were identified across lineages, which suggests that there are no shared pathways for collateral sensitivity and resistance across our lineages; these mutations seem to arise uniquely from within their own lineages based on the delivered antibiotic. Thus, it appears while collateral sensitivity does exist, it can be generated through multiple different pathways and multiple loci. Additional or extended studies would shed light on the different pathways.

Most of our mutations identified were indels and not SNPs. When totaling up all the verified mutations across all our lines there were a total of 562 mutations. Of those 562 mutations, only 49 were SNP mutations. Generally, indel mutation rates are lower in bacteria when compared to substitution mutations, but indels have a significantly higher impact on gene viability [79], instantly disrupting the reading frame, increasing substitution rates in flanking regions [116], and can lead to total gene failure. The large ratio of indels to SNPs suggests that natural selection is greatly influencing the fate of indel mutations, and that sensitivity (and resistance) is rapidly acquired.

The next step in this process is to genetically edit *Burkholderia sp.* to become sensitive to antibiotics. Genetic editing has been performed in *B. pseudomallei* and other *B. species* and these methods can be used to edit the clinical strains described in this manuscript. The perfect flippers are the most likely candidate for editing. In addition to the perfect flipper loci described above, there are also hypothetical proteins and transcription factors that alternate during flipping. These

mutations are also potential candidates for genetic engineering to test for loci that confer collateral sensitivity.

In summary, this work provides a genetic profile for *Burkholderia sp.* that can be used to identify when a *Burkholderia* infection has reached resistance and sensitivity. This list of markers can be used to track whether infections are susceptible to antibiotic treatment and can be used to genetically edit *Bcc* strains for antibiotic susceptibility.

Chapter 6: Conclusions and Future work

Conclusions

In this research, we desired an alternative method for conducting mutation accumulation studies. We initially conducted them per tradition, which was lengthy, tedious, and generated a significant amount of waste in the lab, as well as space occupation. With the rise in accessibility to microfluidic devices, and both 3D printing and PDMS materials, a solution was soon identified. Over the course of these projects, a successful fleet of microfluidic chips has been designed, fabricated, and tested to ensure that it meets the standards required for mutation accumulation studies. While this process also took a considerable amount of time, testing was necessary to successfully identify any flaws in experimental design or protocol which could lead to sub optimal output from each chip. Now we can confidently say that we have a chip that can generate a successful bottleneck and can also perform for extended periods of time with minimal interaction.

A secondary feature that was able to be developed to our microfluidics chips due to the nature of their fabrication is a high degree of customization. Since these chips were designed with a multitude of applications in mind, they can be modified rapidly in order to be directly customized to any desired experiment. Each component of the microfluidic chip design can be readily swapped out for an alternative at any point in the design process, which ultimately provides significant range to the potential applications for the chip. With access to some of the highest quality printers on the market, these chips can also be produced and deployed in a single

day, many designs taking less than 5 hours to print. While a particular experiment may not have generated the desired results, by going through the experimental process, as well as all the testing that led us to this step, we have successfully created a microfluidic chip that can replace traditional mutation accumulation study protocol. These microfluidic chip designs are also highly accessible to anyone without needing to develop a high level of understanding of microfluidics.

With the study conducted on collateral sensitivity with *Burkholderia multivorans*, we were able to identify candidate genes which could be key contributors to antibiotic resistance and sensitivity. In addition to identifying known genes which are already linked to the development of antibiotic resistance and sensitivity, we found unique "flipping" mutations at specific nucleotide positions which perfectly match the flipping of antibiotic sensitivities between parent and child samples. From these flipping genes, we can gain a better understanding of potential gene interactions, as well as target sites for future medication development.

Future Work

With the successful creation of our microfluidic devices, the next steps will be to implement them in a variety of studies. We are currently looking to attain a sample of miss-match repair deficient *Salmonella*, and once acquired, the same experimental process can be conducted. Once this study is complete, we could study the effects on fitness that the mutations generated possess. The protocols for this procedure are already in place as they have been attempted once before. Additionally, these microfluidic chips can be used in similar protocols to test a range of other less studied organisms, such as bacteria that cannot be grown on solid media, extremophiles for example. With the durability and tolerance to heat that the resin

material has, the microfluidic chip can be run under various conditions which are required to house and grow different bacteria. The final goal of the microfluidic chip would be complete automation, so that it could be placed in a more hazardous environment such as the biosafety level 3 laboratory and help minimize human contact time within.

Additional studies could be conducted with microfluidic chips which includes horizontal gene transfer experiments. Horizontal gene transfer describes the ability in which bacteria can digest environmental DNA and incorporate aspects of the digested DNA into their own genome. These studies would help quantify the rates at which horizontal gene transfer takes place within a bacterial population. The protocol would not be too dissimilar to previously established protocols using our microfluidic chip. The process would simply involve flowing DNA laced media into the chip and collecting the cells as one would normally. At regular time intervals cells could be sequenced to detect when the DNA within the media has been successfully incorporated into the bacterial genome. With the presence of the bottlenecking feature of our microfluidic chips we would be studying these with limited influence of selective forces on the bacteria.

REFERENCES

1. Halligan, D. and P. Keightley, *Spontaneous Mutation Accumulation Studies in Evolutionary Genetics.* Annu. Rev. Ecol. Evol. Syst, 2009. **40**: p. 151-72.
2. Robert, L., et al., *Mutation dynamics and fitness effects followed in single cells.* Science, 2018. **359**(6381): p. 1283-1286.
3. Martinez, J.L. and F. Baquero, *Mutation frequencies and antibiotic resistance.* Antimicrob Agents Chemother, 2000. **44**(7): p. 1771-7.
4. Ho, C.Y. and C.A. MacRae, *Defining the Pathogenicity of DNA Sequence Variation.* Circulation: Cardiovascular Genetics, 2009. **2**(2): p. 95-97.
5. Kochański, A., *Pathogenic mutations and non-pathogenic DNA polymorphisms in the most common neurodegenerative disorders.* Folia Neuropathol, 2007. **45**(4): p. 164-9.
6. Sun, H. and G. Yu, *New insights into the pathogenicity of non-synonymous variants through multi-level analysis.* Scientific Reports, 2019. **9**(1): p. 1667.
7. Barton, N.H., *Mutation and the evolution of recombination.* Philos Trans R Soc Lond B Biol Sci, 2010. **365**(1544): p. 1281-94.
8. Hershberg, R., *Mutation--The Engine of Evolution: Studying Mutation and Its Role in the Evolution of Bacteria.* Cold Spring Harb Perspect Biol, 2015. **7**(9): p. a018077.
9. Loewe, L. and W.G. Hill, *The population genetics of mutations: good, bad and indifferent.* Philos Trans R Soc Lond B Biol Sci, 2010. **365**(1544): p. 1153-67.
10. Jackson, M., et al., *The genetic basis of disease.* Essays Biochem, 2018. **62**(5): p. 643-723.
11. Růžička, M., et al., *DNA mutation motifs in the genes associated with inherited diseases.* PLOS ONE, 2017. **12**(8): p. e0182377.
12. Bromham, L. and D. Penny, *The modern molecular clock.* Nat Rev Genet, 2003. **4**(3): p. 216-24.
13. Ho, S., *The molecular clock and estimating species divergence.* Nature Education, 2008. **1**(1): p. 1-2.
14. Gordo, I., L. Perfeito, and A. Sousa, *Fitness effects of mutations in bacteria.* J Mol Microbiol Biotechnol, 2011. **21**(1-2): p. 20-35.
15. Mehlhoff, J.D., et al., *Collateral fitness effects of mutations.* Proc Natl Acad Sci U S A, 2020. **117**(21): p. 11597-11607.
16. Chevallereau, A., et al., *The effect of bacterial mutation rate on the evolution of CRISPR-Cas adaptive immunity.* Philosophical Transactions of the Royal Society B: Biological Sciences, 2019. **374**(1772): p. 20180094.
17. Heilbron, K., et al., *Fitness Is Strongly Influenced by Rare Mutations of Large Effect in a Microbial Mutation Accumulation Experiment.* Genetics, 2014. **197**(3): p. 981-990.
18. Katju, V. and U. Bergthorsson, *Old Trade, New Tricks: Insights into the Spontaneous Mutation Process from the Partnering of Classical Mutation Accumulation Experiments with High-Throughput Genomic Approaches.* Genome Biology and Evolution, 2019. **11**(1): p. 136-165.

19. Keightley, P.D., et al., *Analysis of the genome sequences of three Drosophila melanogaster spontaneous mutation accumulation lines.* Genome Research, 2009. **19**(7): p. 1195-1201.
20. Sung, W., et al., *Asymmetric Context-Dependent Mutation Patterns Revealed through Mutation–Accumulation Experiments.* Molecular Biology and Evolution, 2015. **32**(7): p. 1672-1683.
21. Lynch, M., *Evolution of the mutation rate.* Trends in Genetics, 2010. **26**(8): p. 345-352.
22. Stewart, E.J., *Growing Unculturable Bacteria.* Journal of Bacteriology, 2012. **194**(16): p. 4151-4160.
23. Lenski, R.E., *Experimental evolution and the dynamics of adaptation and genome evolution in microbial populations.* The ISME Journal, 2017. **11**(10): p. 2181-2194.
24. Bai, Y., et al., *Applications of Microfluidics in Quantitative Biology.* Biotechnol J, 2018. **13**(5): p. e1700170.
25. Hershberg, R., *Mutation—The Engine of Evolution: Studying Mutation and Its Role in the Evolution of Bacteria: Figure 1.* Cold Spring Harbor Perspectives in Biology, 2015. **7**(9): p. a018077.
26. Thompson, A.M., et al., *Microfluidics for single-cell genetic analysis.* 2014. **14**(17): p. 3135.
27. Raj M, K. and S. Chakraborty, *PDMS microfluidics: A mini review.* Journal of Applied Polymer Science, 2020. **137**(27): p. 48958.
28. Fu, Y.-X. and H. Huai, *Estimating Mutation Rate: How to Count Mutations?* Genetics, 2003. **164**(2): p. 797-805.
29. Charlesworth, B., *The effects of deleterious mutations on evolution at linked sites.* Genetics, 2012. **190**(1): p. 5-22.
30. Bao, K., R.H. Melde, and N.P. Sharp, *Are mutations usually deleterious? A perspective on the fitness effects of mutation accumulation.* Evol Ecol, 2022. **36**(5): p. 753-766.
31. Luria, S.E. and M. Delbrück, *Mutations of Bacteria from Virus Sensitivity to Virus Resistance.* Genetics, 1943. **28**(6): p. 491-511.
32. Foster, P.L., *Methods for Determining Spontaneous Mutation Rates*. 2006, Elsevier. p. 195-213.
33. de Jong, N.W.M., et al., *Fluorescent reporters for markerless genomic integration in Staphylococcus aureus.* Scientific Reports, 2017. **7**(1): p. 43889.
34. Berger, J., et al., *Secreted placental alkaline phosphatase: a powerful new quantitative indicator of gene expression in eukaryotic cells.* Gene, 1988. **66**(1): p. 1-10.
35. Brasier, A.R., J.E. Tate, and J.F. Habener, *Optimized use of the firefly luciferase assay as a reporter gene in mammalian cell lines.* BioTechniques, 1989. **7**(10): p. 1116-1122.
36. Chartrand, P., et al., *Structural elements required for the localization of ASH1 mRNA and of a green fluorescent protein reporter particle in vivo.* Current Biology, 1999. **9**(6): p. 333-338.
37. Kim, K.-W., et al., *β-Glucuronidase as Reporter Gene*, in *Arabidopsis Protocols*, J. Salinas and J.J. Sanchez-Serrano, Editors. 2006, Humana Press: Totowa, NJ. p. 263-273.
38. MacGregor, G.R., et al., *Use of Escherichiu coli (E. coli) lacZ (β-Galactosidase) as a Reporter Gene*, in *Gene Transfer and Expression Protocols*, E.J. Murray, Editor. 1991, Humana Press: Totowa, NJ. p. 217-235.
39. Zhu, Y.O., et al., *Precise estimates of mutation rate and spectrum in yeast.* Proceedings of the National Academy of Sciences, 2014. **111**(22): p. E2310-E2318.

40. Donald F Conrad, et al., *Variation in genome-wide mutation rates within and between human families.* Nature Genetics, 2011. **43**(7): p. 712-714.
41. Sasani, T.A., et al., *Large, three-generation human families reveal post-zygotic mosaicism and variability in germline mutation accumulation.* eLife, 2019. **8**: p. e46922.
42. Kryazhimskiy, S. and J.B. Plotkin, *The Population Genetics of dN/dS.* PLOS Genetics, 2008. **4**(12): p. e1000304.
43. Kryazhimskiy, S. and J.B. Plotkin, *The population genetics of dN/dS.* PLoS Genet, 2008. **4**(12): p. e1000304.
44. McVean, G.A. and J. Vieira, *Inferring parameters of mutation, selection and demography from patterns of synonymous site evolution in Drosophila.* Genetics, 2001. **157**(1): p. 245-57.
45. Lande, R., *Natural Selection and Random Genetic Drift in Phenotypic Evolution.* Evolution, 1976. **30**(2): p. 314-334.
46. Drake, J.W., *Contrasting Mutation Rates from Specific-Locus and Long-Term Mutation-Accumulation Procedures.* G3 Genes|Genomes|Genetics, 2012. **2**(4): p. 483-485.
47. Konrad, A., et al., *Mitochondrial Mutation Rate, Spectrum and Heteroplasmy in Caenorhabditis elegans Spontaneous Mutation Accumulation Lines of Differing Population Size.* Molecular Biology and Evolution, 2017: p. msx051.
48. Flynn, J.M., et al., *Spontaneous Mutation Accumulation inDaphnia pulexin Selection-Free vs. Competitive Environments.* Molecular Biology and Evolution, 2017. **34**(1): p. 160-173.
49. Jay, P., et al., *Mutation accumulation in chromosomal inversions maintains wing pattern polymorphism in a butterfly*. 2019, Cold Spring Harbor Laboratory.
50. Valesano, A.L., et al., *Temporal dynamics of SARS-CoV-2 mutation accumulation within and across infected hosts.* PLOS Pathogens, 2021. **17**(4): p. e1009499.
51. Jager, M., et al., *Measuring mutation accumulation in single human adult stem cells by whole-genome sequencing of organoid cultures.* Nature Protocols, 2018. **13**(1): p. 59-78.
52. Rodríguez, J.A., et al., *Antagonistic pleiotropy and mutation accumulation influence human senescence and disease.* Nature Ecology & Evolution, 2017. **1**(3): p. 0055.
53. Baer, C.F., M.M. Miyamoto, and D.R. Denver, *Mutation rate variation in multicellular eukaryotes: causes and consequences.* Nat Rev Genet, 2007. **8**(8): p. 619-31.
54. Long, H., et al., *Evolutionary determinants of genome-wide nucleotide composition.* Nat Ecol Evol, 2018. **2**(2): p. 237-240.
55. Shadrin, A.A. and D.V. Parkhomchuk, *Drake's rule as a consequence of approaching channel capacity.* Naturwissenschaften, 2014. **101**(11): p. 939-954.
56. Drake, J.W., *A constant rate of spontaneous mutation in DNA-based microbes.* Proc Natl Acad Sci U S A, 1991. **88**(16): p. 7160-4.
57. Sung, W., et al., *Drift-barrier hypothesis and mutation-rate evolution.* Proceedings of the National Academy of Sciences, 2012. **109**(45): p. 18488-18492.
58. Sung, W., et al., *Evolution of the Insertion-Deletion Mutation Rate Across the Tree of Life.* G3: Genes|Genomes|Genetics, 2016. **6**(8): p. 2583-2591.
59. Drake, J.W., *A constant rate of spontaneous mutation in DNA-based microbes.* Proceedings of the National Academy of Sciences, 1991. **88**(16): p. 7160-7164.
60. Lynch, M., et al., *The repatterning of eukaryotic genomes by random genetic drift.* Annu Rev Genomics Hum Genet, 2011. **12**: p. 347-66.

61. Sung, W., et al., *Extraordinary genome stability in the ciliate Paramecium tetraurelia.* Proceedings of the National Academy of Sciences, 2012. **109**(47): p. 19339-19344.
62. Sniegowski, P. and Y. Raynes, *Mutation Rates: How Low Can You Go?* Current Biology, 2013. **23**(4): p. R147-R149.
63. Waheed, S., et al., *3D printed microfluidic devices: enablers and barriers.* Lab on a Chip, 2016. **16**(11): p. 1993-2013.
64. Weisgrab, G., A. Ovsianikov, and P.F. Costa, *Functional 3D Printing for Microfluidic Chips.* Advanced Materials Technologies, 2019. **4**(10).
65. Gurung, J.P., M. Gel, and M.A.B. Baker, *Microfluidic techniques for separation of bacterial cells via taxis.* Microb Cell, 2020. **7**(3): p. 66-79.
66. Sowa, Y. and R.M. Berry, *Bacterial flagellar motor.* Q Rev Biophys, 2008. **41**(2): p. 103-32.
67. Darnton, N.C., et al., *On torque and tumbling in swimming Escherichia coli.* J Bacteriol, 2007. **189**(5): p. 1756-64.
68. Lauga, E., *Bacterial Hydrodynamics.* Annual Review of Fluid Mechanics, 2016. **48**(1): p. 105-130.
69. Pranzo, D., et al., *Extrusion-Based 3D Printing of Microfluidic Devices for Chemical and Biomedical Applications: A Topical Review.* Micromachines, 2018. **9**(8): p. 374.
70. Figueroa-Morales, N., et al., *Living on the edge: transfer and traffic of E. coli in a confined flow.* Soft Matter, 2015. **11**(31): p. 6284-6293.
71. Mathijssen, A.J.T.M., et al., *Oscillatory surface rheotaxis of swimming E. coli bacteria.* Nature Communications, 2019. **10**(1).
72. Rusconi, R., J.S. Guasto, and R. Stocker, *Bacterial transport suppressed by fluid shear.* Nature Physics, 2014. **10**(3): p. 212-217.
73. Koldaeva, A., et al., *Population genetics in microchannels*. 2021.
74. Yang, D., et al., *Analysis of Factors Limiting Bacterial Growth in PDMS Mother Machine Devices.* Frontiers in Microbiology, 2018. **9**.
75. Li, H. and R. Durbin, *Fast and accurate short read alignment with Burrows-Wheeler transform.* Bioinformatics, 2009. **25**(14): p. 1754-60.
76. Li, H., et al., *The Sequence Alignment/Map format and SAMtools.* Bioinformatics, 2009. **25**(16): p. 2078-2079.
77. Lynch, M., et al., *A genome-wide view of the spectrum of spontaneous mutations in yeast.* Proc Natl Acad Sci U S A, 2008. **105**(27): p. 9272-7.
78. Ossowski, S., et al., *The rate and molecular spectrum of spontaneous mutations in Arabidopsis thaliana.* Science, 2010. **327**(5961): p. 92-4.
79. Sung, W., et al., *Evolution of the Insertion-Deletion Mutation Rate Across the Tree of Life.* G3 Genes|Genomes|Genetics, 2016. **6**(8): p. 2583-2591.
80. Cingolani, P., et al., *Using Drosophila melanogaster as a Model for Genotoxic Chemical Mutational Studies with a New Program, SnpSift.* Front Genet, 2012. **3**: p. 35.
81. Kerem, B., et al., *Identification of the cystic fibrosis gene: genetic analysis.* Science, 1989. **245**(4922): p. 1073-80.
82. Spoonhower, K.A. and P.B. Davis, *Epidemiology of Cystic Fibrosis.* Clin Chest Med, 2016. **37**(1): p. 1-8.
83. Li, C., et al., *ATPase activity of the cystic fibrosis transmembrane conductance regulator.* J Biol Chem, 1996. **271**(45): p. 28463-8.

84. *Foundation, C.F. Patient Registry Annual Data Report. 2021 https://www.cff.org/medical-professionals/patient-registry.*
85. Pranke, I., et al., *Emerging Therapeutic Approaches for Cystic Fibrosis. From Gene Editing to Personalized Medicine.* Front Pharmacol, 2019. **10**: p. 121.
86. Berical, A., et al., *Challenges Facing Airway Epithelial Cell-Based Therapy for Cystic Fibrosis.* Frontiers in Pharmacology, 2019. **10**.
87. Kidd, T.J., et al., *Defining antimicrobial resistance in cystic fibrosis.* Journal of Cystic Fibrosis, 2018. **17**(6): p. 696-704.
88. Starkey, M., et al., *Pseudomonas aeruginosa rugose small-colony variants have adaptations that likely promote persistence in the cystic fibrosis lung.* J Bacteriol, 2009. **191**(11): p. 3492-503.
89. Welch, W.J., *Role of quality control pathways in human diseases involving protein misfolding.* Semin Cell Dev Biol, 2004. **15**(1): p. 31-8.
90. Egan, M.E., *Genetics of Cystic Fibrosis: Clinical Implications.* Clin Chest Med, 2016. **37**(1): p. 9-16.
91. Sawicki, G.S., et al., *Sustained Benefit from ivacaftor demonstrated by combining clinical trial and cystic fibrosis patient registry data.* Am J Respir Crit Care Med, 2015. **192**(7): p. 836-42.
92. Armougom, F., et al., *Microbial diversity in the sputum of a cystic fibrosis patient studied with 16S rDNA pyrosequencing.* Eur J Clin Microbiol Infect Dis, 2009. **28**(9): p. 1151-4.
93. Windels, E.M., et al., *Bacterial persistence promotes the evolution of antibiotic resistance by increasing survival and mutation rates.* Isme j, 2019. **13**(5): p. 1239-1251.
94. Colclough, A., et al., *Patterns of cross-resistance and collateral sensitivity between clinical antibiotics and natural antimicrobials.* Evol Appl, 2019. **12**(5): p. 878-887.
95. Lee, I.M., et al., *Effect of physical inactivity on major non-communicable diseases worldwide: an analysis of burden of disease and life expectancy.* Lancet, 2012. **380**(9838): p. 219-29.
96. Sung, W., et al., *Evolution of the Insertion-Deletion Mutation Rate Across the Tree of Life.* G3 (Bethesda), 2016. **6**(8): p. 2583-91.
97. Meletis, G., *Carbapenem resistance: overview of the problem and future perspectives.* Ther Adv Infect Dis, 2016. **3**(1): p. 15-21.
98. Asadi, A., et al., *Minocycline, focus on mechanisms of resistance, antibacterial activity, and clinical effectiveness: Back to the future.* Journal of Global Antimicrobial Resistance, 2020. **22**: p. 161-174.
99. Jacoby, G.A., *Mechanisms of Resistance to Quinolones.* Clinical Infectious Diseases, 2005. **41**(Supplement_2): p. S120-S126.
100. Rhodes, K.A. and H.P. Schweizer, *Antibiotic resistance in Burkholderia species.* Drug Resist Updat, 2016. **28**: p. 82-90.
101. Kemnic TR, C.M., *Trimethoprim Sulfamethoxazole.* StatPearls Publishing, 2023.
102. Chantratita, N., et al., *Antimicrobial resistance to ceftazidime involving loss of penicillin-binding protein 3 in Burkholderia pseudomallei.* Proceedings of the National Academy of Sciences, 2011. **108**(41): p. 17165-17170.
103. Sharma, A.K., et al., *Bacterial Virulence Factors: Secreted for Survival.* Indian J Microbiol, 2017. **57**(1): p. 1-10.

104. Beceiro, A., M. Tomás, and G. Bou, *Antimicrobial resistance and virulence: a successful or deleterious association in the bacterial world?* Clin Microbiol Rev, 2013. **26**(2): p. 185-230.
105. Iyer, R., et al., *A biological role for prokaryotic ClC chloride channels.* Nature, 2002. **419**(6908): p. 715-718.
106. Hughes, K.T. and K. Mathee, *The anti-sigma factors.* Annu Rev Microbiol, 1998. **52**: p. 231-86.
107. Matilla, M.A. and T. Krell, *Noncanonical Sensing Mechanisms for Bacillus subtilis Chemoreceptors.* Journal of Bacteriology, 2022. **204**(4): p. e00027-22.
108. Amare, B., et al., *LigD: A Structural Guide to the Multi-Tool of Bacterial Non-Homologous End Joining.* Front Mol Biosci, 2021. **8**: p. 787709.
109. Gong, C., et al., *Mechanism of nonhomologous end-joining in mycobacteria: a low-fidelity repair system driven by Ku, ligase D and ligase C.* Nat Struct Mol Biol, 2005. **12**(4): p. 304-12.
110. Bryant, J.A., et al., *Structure of dual BON-domain protein DolP identifies phospholipid binding as a new mechanism for protein localisation.* eLife, 2020. **9**: p. e62614.
111. Kuwahara, Y., et al., *The solution structure of the C-terminal domain of NfeD reveals a novel membrane-anchored OB-fold.* Protein Sci, 2008. **17**(11): p. 1915-24.
112. Chan, G.F., N.A.A. Rashid, and A.R.M. Yusoff, *Expression, purification and characterization of flavin reductase from Citrobacter freundii A1.* Annals of Microbiology, 2013. **63**(1): p. 343-351.
113. Choi, U. and C.-R. Lee, *Distinct Roles of Outer Membrane Porins in Antibiotic Resistance and Membrane Integrity in Escherichia coli.* Frontiers in Microbiology, 2019. **10**.
114. Welsh, M.A., et al., *Identification of a Functionally Unique Family of Penicillin-Binding Proteins.* Journal of the American Chemical Society, 2017. **139**(49): p. 17727-17730.
115. Stubenrauch, C.J., et al., *A noncanonical chaperone interacts with drug efflux pumps during their assembly into bacterial outer membranes.* PLOS Biology, 2022. **20**(1): p. e3001523.
116. Williams, L.E. and J.J. Wernegreen, *Sequence context of indel mutations and their effect on protein evolution in a bacterial endosymbiont.* Genome Biol Evol, 2013. **5**(3): p. 599-605.